Green's functions and boundary element analysis for bimaterials with soft and stiff planar interfaces under plane elastostatic deformations

E. L. Chen and W. T. Ang*
Division of Engineering Mechanics,
School of Mechanical and Aerospace Engineering,
Nanyang Technological University,
Singapore

To appear in Engineering Analysis with Boundary Elements
DOI:10.1016/ j.enganabound.2013.11.014.

Abstract

Plane elastostatic Green's functions satisfying relevant conditions on soft and stiff planar interfaces between two dissimilar anisotropic half spaces under elastostatic deformations are explicitly derived with the aid of the Fourier integral transformation technique. The Green's functions are applied to obtain special boundary integral equations for the deformation of a bimaterial with an imperfect planar interface that is either soft or stiff. The boundary integral equations do not contain any integral over the imperfect interface. They are used to obtain a boundary element procedure for determining the displacements and stresses in the bimaterial. The numerical procedure does not require the interface to be discretized into elements.

* Author for correspondence (E-mail: MWTANG@ntu.edu.sg).

1 Introduction

Two dissimilar materials joined by an extremely thin layer of material sandwiched in between them may be modeled as a bimaterial with an interface in the form of a surface. The boundary conditions to impose on the interface, which may influence the overall mechanical behaviors of the bimaterial, depend on the elastic properties of the thin layer between the two materials and may be derived using asymptotic analysis as explained in Benveniste and Miloh [4].

In many research articles, such as Ang and Park [2], Fenner [10], Kattis and Mavroyannis [15] and Yu *et al.* [19], the interface is taken to be perfect, that is, the dissimilar materials are assumed to be bonded in such that a way that the displacements and the traction stresses are continuous on the interface. Nevertheless, if the thin layer between the dissimilar materials is extremely soft or stiff, or if the interface contains micro-cracks or rigid micro-inclusions, the perfect interface model may not be suitable for analyzing the deformation of the bimaterial. This explains why the analysis of imperfect interfaces has attracted the attention of many researchers (see, for example, Achenbach and Zhu [1], Fan and Wang [9], Hashin [13] and Sudak [17]).

Most studies on imperfect interfaces deal with compliant or soft interfaces which are modeled as distributions of springs. In the spring model, the displacements may jump across opposite sides of a soft interface but traction stresses are continuous on the interface, and the traction stresses on the interface are linearly related to the displacement jumps. For stiff interfaces considered in Benveniste and Miloh [4] and Hashin [14], the displacements are continuous on a stiff interface but the traction stresses may exhibit a jump across opposite sides of the interface. Relatively few papers on the analysis of stiff interfaces may be found in the literature.

In the present paper, plane elastostatic Green's functions satisfying the relevant conditions on imperfect soft and stiff planar interfaces between two dissimilar anisotropic half spaces under elastostatic deformations are explicitly derived with the aid of the Fourier integral transformation technique. The Green's functions are applied to obtain special boundary integral equations for the deformation of a bimaterial with an imperfect planar interface that is either soft or stiff. The boundary integral equations do not contain any integral over the imperfect interface. They are used to obtain a boundary element procedure for determining the displacements and stresses in the bimaterial. The numerical procedure does not require the interface to be discretized into elements.

Earlier works on plane elastostatic Green's functions for imperfect planar interfaces in bimaterials may be found in Berger and Tewary [5] and Sudak and Wang [18]. In [5], the displacement jumps across opposite sides of the imperfect soft interface are assumed known a priori and the Green's function is chosen to have explicitly prescribed displacement jumps. The Green's function in [18] satisfies a specific case of the interface conditions in the spring model for imperfect soft interfaces. A more general form of the soft interface conditions is considered in the present paper.

It may be worth mentioning here that numerical methods based on boundary integral equations have received considerable attention in the engineering analysis of multilayered materials and composite materials. Readers interested in recent development of such boundary element approaches may refer to Gu *et al.* [11]-[12].

2 Imperfect soft and stiff planar interfaces

Referring to a Cartesian coordinate system $Ox_1x_2x_3$, consider two anisotropic elastic half spaces $x_2 > \delta$ and $x_2 < 0$ with an anisotropic elastic layer of thickness δ sandwiched in between them. The elastic layer $0 < x_2 < \delta$ is denoted by $R^{(0)}$ and the elastic half spaces $x_2 > \delta$ and $x_2 < 0$ by $R^{(1)}$ and $R^{(2)}$ respectively. The elastic moduli of the region $R^{(p)}$ is given by $c^{(p)}_{ijk\ell}$ $(p = 0, 1, 2)$. Refer to Figure 1 for a sketch of the multilayered elastic space on the Ox_1x_2 plane.

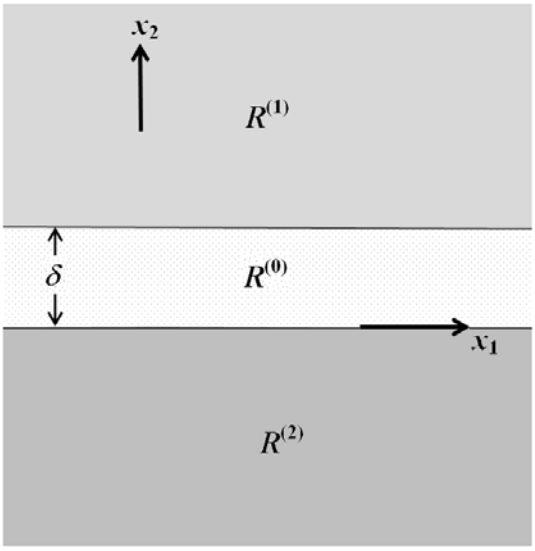

Figure 1. Two anisotropic elastic half spaces $x_2 > \delta$ and $x_2 < 0$ with an anisotropic elastic layer of thickness δ sandwiched in between them.

The multilayered elastic space in Figure 1 undergoes a plane elastostatic deformation such that the elastic displacement and stress fields are functions of x_1 and x_2 only. The continuity conditions imposed on the planes $x_2 = 0$

and $x_2 = \delta$ are given by

$$\left.\begin{array}{rcl} u_i^{(0)}(x_1, \delta^-) & = & u_i^{(1)}(x_1, \delta^+) \\ \sigma_{i2}^{(0)}(x_1, \delta^-) & = & \sigma_{i2}^{(1)}(x_1, \delta^+) \\ u_i^{(0)}(x_1, 0^+) & = & u_i^{(2)}(x_1, 0^-) \\ \sigma_{i2}^{(0)}(x_1, 0^+) & = & \sigma_{i2}^{(2)}(x_1, 0^-) \end{array}\right\} \text{ for } -\infty < x_1 < \infty, \tag{1}$$

where $u_i^{(p)}$ and $\sigma_{ij}^{(p)}$ are respectively the dispapcements and stresses in the region $R^{(p)}$.

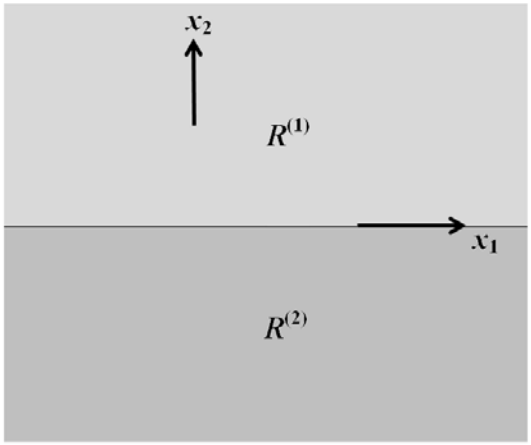

Figure 2. Two dissimilar elastic half spaces joined along $x_2 = 0$.

We are interested in modeling the sandwiched layer $R^{(0)}$ as a line interface on the x_1 axis of the Ox_1x_2 plane for the limiting case in which the thickness δ tends to zero. A geometrical sketch of the layered elastic space for the vanishing layer replaced by the planar interface on the $x_2 = 0$ is shown in Figure 2.

If the elastic moduli $c_{ijk\ell}^{(0)}$ in the layer $R^{(0)}$ either vanish or become un-

bounded as δ tends to zero, then the perfect interface conditions

$$\left.\begin{array}{rcl} u_i^{(1)}(x_1,0^+) & = & u_i^{(2)}(x_1,0^-) \\ \sigma_{i2}^{(1)}(x_1,0^+) & = & \sigma_{i2}^{(2)}(x_1,0^-) \end{array}\right\} \text{ for } -\infty < x_1 < \infty, \tag{2}$$

may not necessarily hold for the bimaterial in Figure 2.

The asymptotic analysis in Benveniste and Miloh [4] may be applied to derive conditions on $x_2 = 0$ (in the limit as δ tends to zero) for soft and stiff interfaces as explained in Subsections 2.1 and 2.2 below. For the asymptotic analysis, the displacement and the stress fields in $R^{(1)}$ and $R^{(2)}$ as well as the partial derivatives of those fields with respect to x_i are assumed to be $O(1)$ (for small δ) on the interface $x_2 = 0$ and the Taylor series is used to write

$$u_i^{(0)}(x_1,\delta^-) - u_i^{(0)}(x_1,0^+) \;=\; \delta \left.\frac{\partial u_i^{(0)}}{\partial x_2}\right|_{x_2=0^+} + \sum_{m=2}^{\infty} \frac{\delta^m}{m!} \left.\frac{\partial^m u_i^{(0)}}{\partial x_2^m}\right|_{x_2=0^+}, \tag{3}$$

and

$$\sigma_{i2}^{(0)}(x_1,\delta^-) - \sigma_{i2}^{(0)}(x_1,0^+) \;=\; \delta \left.\frac{\partial \sigma_{i2}^{(0)}}{\partial x_2}\right|_{x_2=0^+} + \sum_{m=2}^{\infty} \frac{\delta^m}{m!} \left.\frac{\partial^m \sigma_{i2}^{(0)}}{\partial x_2^m}\right|_{x_2=0^+}. \tag{4}$$

2.1 Soft interface conditions

The soft interface conditions are obtained if the elastic moduli $c_{ijk\ell}^{(0)}$ in the layer $R^{(0)}$ decreases to zero as δ tends to zero in accordance with

$$c_{ijk\ell}^{(0)} = \delta c_{ijk\ell}^{(\text{soft})}, \tag{5}$$

where $c_{ijk\ell}^{(\text{soft})}$ are constants independent of δ.

From the equilibrium equations

$$\frac{\partial \sigma_{ij}^{(0)}}{\partial x_j} = 0 \text{ in } R^{(0)}, \tag{6}$$

and the generalized Hooke's law

$$\sigma_{ij}^{(0)} = c_{ijk\ell}^{(0)} \frac{\partial u_k^{(0)}}{\partial x_\ell}, \tag{7}$$

we may write

$$\delta \left. \frac{\partial \sigma_{i2}^{(0)}}{\partial x_2} \right|_{x_2=0^+} = -\delta \left. \left[c_{i1k1}^{(0)} \frac{\partial^2 u_k^{(0)}}{\partial x_1^2} + c_{i1k2}^{(0)} \frac{\partial^2 u_k^{(0)}}{\partial x_1 \partial x_2} \right] \right|_{x_2=0^+}. \tag{8}$$

Note that the Einstenian convention of summing over a repeated index is assumed here for lowercase Latin subscripts which take the values 1 and 2.

From $u_i^{(0)}(x_1, 0^+) = u_i^{(2)}(x_1, 0^-)$ (in the third line of (1)), (8) may be rewritten as

$$\delta \left. \frac{\partial \sigma_{i2}^{(0)}}{\partial x_2} \right|_{x_2=0^+} = -\delta c_{i1k1}^{(0)} \left. \frac{\partial^2 u_k^{(2)}}{\partial x_1^2} \right|_{x_2=0^-} - \delta c_{i1k2}^{(0)} \left. \frac{\partial^2 u_k^{(0)}}{\partial x_1 \partial x_2} \right|_{x_2=0^+}. \tag{9}$$

Using $\sigma_{i2}^{(0)}(x_1, 0^+) = \sigma_{i2}^{(2)}(x_1, 0^-)$ (in the fourth line of (1)) and (7), we find that

$$c_{i2k2}^{(0)} \left. \frac{\partial u_k^{(0)}}{\partial x_2} \right|_{x_2=0^+} = -c_{i2k1}^{(0)} \left. \frac{\partial u_k^{(2)}}{\partial x_1} \right|_{x_2=0^-} + \sigma_{i2}^{(2)}(x_1, 0^-), \tag{10}$$

and hence

$$c_{i2k2}^{(0)} \left. \frac{\partial^2 u_k^{(0)}}{\partial x_1 \partial x_2} \right|_{x_2=0^+} = -c_{i2k1}^{(0)} \left. \frac{\partial^2 u_k^{(2)}}{\partial x_1^2} \right|_{x_2=0^-} + \left. \frac{\partial \sigma_{i2}^{(2)}}{\partial x_1} \right|_{x_2=0^-}. \tag{11}$$

Since $u^{(2)}$ and $\sigma_{i2}^{(2)}$ are assumed to be $O(1)$ (for small δ) and $c_{ijk\ell}^{(0)}$ is given by (5), the right hand side of (11) is $O(1)$ and (9) implies that the first order partial derivative of $\sigma_{i2}^{(0)}$with respect to x_2 at $x_2 = 0^+$ is $O(1)$. It follows that (4) reduces to

$$\sigma_{i2}^{(1)}(x_1, 0^+) = \sigma_{i2}^{(2)}(x_1, 0^-), \tag{12}$$

as δ tends to zero.

Similarly, from (5) and (10), as δ approaches zero, (3) reduces to

$$\lambda_{ik}[u_k^{(1)}(x_1, 0^+) - u_k^{(2)}(x_1, 0^-)] = \sigma_{i2}^{(2)}(x_1, 0^-), \tag{13}$$

where $\lambda_{ik} = c_{i2k2}^{(\text{soft})}$.

To summarize, the soft interface conditions are given by (12) and (13). The conditions may also be used to describe an interface that is damaged by a distribution of micro-cracks or micro-voids.

2.2 Stiff interface conditions

For the stiff interface conditions, the elastic moduli $c_{ijk\ell}^{(0)}$ of the vanishing layer $R^{(0)}$ are taken to be given by

$$c_{ijk\ell}^{(0)} = \frac{1}{\delta} c_{ijk\ell}^{(\text{stiff})}, \tag{14}$$

where $c_{ijk\ell}^{(\text{stiff})}$ are constants independent of δ.

Since $u^{(2)}$ and $\sigma_{i2}^{(2)}$ are assumed to be $O(1)$ (for small δ) and $c_{ijk\ell}^{(0)}$ is given by (14), the right hand side of (10) is $O(\delta^{-1})$ and hence the first order partial derivative of $u_k^{(0)}$with respect to x_2 at $x_2 = 0^+$ is $O(1)$. It follows that (3) reduces to

$$u_k^{(2)}(x_1, 0^-) = u_k^{(1)}(x_1, 0^+), \tag{15}$$

as δ tends to zero.

Similarly, (4) together with (1), (8) and (11) gives

$$\sigma_{i2}^{(1)}(x_1, 0^+) - \sigma_{i2}^{(2)}(x_1, 0^-) = -\alpha_{ik} \left. \frac{\partial^2 u_k^{(1)}}{\partial x_1^2} \right|_{x_2 = 0^+}. \tag{16}$$

where

$$\alpha_{ik} = -c_{i1k1}^{(\text{stiff})} + c_{i1p2}^{(\text{stiff})} b_{pj} c_{j2k1}^{(\text{stiff})}, \tag{17}$$

with b_{pi} defined by

$$b_{pi} c_{i2k2}^{(\text{stiff})} = \delta_{pk}. \tag{18}$$

Note that δ_{pk} is the Kronecker-delta.

To summarize, the stiff interface conditions are given by (15) and (16). The conditions may also be used to model an interface containing a distribution of rigid micro-inclusions.

3 Green's functions for planar interfaces

In this section, we derive plane elastostatic Green's functions for imperfect soft and stiff planar interfaces between the anisotropic elastic half spaces in Figure 2. The Green's function for a perfect interface, which is given in Berger and Tewary [6], is also presented here.

The task of deriving the Green's functions for the interfaces requires solving the systems of partial differential equations

$$\begin{aligned} c^{(p)}_{ijk\ell}\frac{\partial^2}{\partial x_j \partial x_\ell}[\Phi_{km}(x_1,x_2;\xi_1,\xi_2)] &= \delta_{im}\delta(x_1-\xi_1,x_2-\xi_2) \\ &\qquad \text{for } (x_1,x_2)\in R^{(p)}\ (p=1,2), \quad (19) \end{aligned}$$

where $\delta(x_1,x_2)$ is the Dirac delta function and $\Phi_{km}(x_1,x_2;\xi_1,\xi_2)$ are the displacement fundamental solutions to be modified to satisfy the relevant far-field and interface conditions.

For the far-field conditions, the stresses $S_{ijm}(x_1,x_2;\xi_1,\xi_2)$ defined by

$$\begin{aligned} S_{ijm}(x_1,x_2;\xi_1,\xi_2) &= c^{(p)}_{ijk\ell}\frac{\partial}{\partial x_\ell}[\Phi_{km}(x_1,x_2;\xi_1,\xi_2)] \\ &\qquad \text{for } (x_1,x_2)\in R^{(p)}\ (p=1,2), \qquad (20) \end{aligned}$$

are required to tend to zero as $x_1^2+x_2^2\to\infty$.

The Green's functions $\Phi_{km}(x_1,x_2;\xi_1,\xi_2)$ are given in (22), (27) and (35) for perfect, soft and stiff interfaces respectively.

3.1 Perfect interface

If the interface between the anisotropic elastic half spaces in Figure 2 is perfect, the interface conditions for the Green's function are given by

$$\left.\begin{array}{l}\Phi_{km}(x_1,0^+;\xi_1,\xi_2)=\Phi_{km}(x_1,0^-;\xi_1,\xi_2)\\ S_{k2m}(x_1,0^+;\xi_1,\xi_2)=S_{k2m}(x_1,0^-;\xi_1,\xi_2)\end{array}\right\}\ \text{for}\ -\infty<x_1<\infty, \tag{21}$$

The solution of (19) satisfying (20) and (21), which is given in Berger and Tewary [6], may be written as

$$\begin{aligned}
&\Phi_{km}^{(\text{perfect})}(x_1,x_2;\xi_1,\xi_2)\\
=\ &\frac{1}{2\pi}\,\text{Re}\{\sum_{\alpha=1}^{2}(H(x_2)H(\xi_2)A_{k\alpha}^{(1)}[N_{\alpha p}^{(1)}\ln(x_1-\xi_1+\tau_\alpha^{(1)}(x_2-\xi_2))\\
&+\sum_{\beta=1}^{2}Q_{\alpha\beta j}^{(1)}\ln(x_1-\xi_1+\tau_\alpha^{(1)}x_2-\overline{\tau}_\beta^{(1)}\xi_2)]d_{pm}^{(1)}\\
&+H(-x_2)H(\xi_2)\sum_{\beta=1}^{2}A_{k\alpha}^{(2)}Q_{\alpha\beta p}^{(2)}d_{pm}^{(1)}\ln(x_1-\xi_1+\tau_\alpha^{(2)}x_2-\tau_\beta^{(1)}\xi_2)\\
&+H(x_2)H(-\xi_2)\sum_{\beta=1}^{2}A_{k\alpha}^{(1)}T_{\alpha\beta p}^{(1)}d_{pm}^{(2)}\ln(x_1-\xi_1+\tau_\alpha^{(1)}x_2-\tau_\beta^{(2)}\xi_2)\\
&+H(-x_2)H(-\xi_2)A_{k\alpha}^{(2)}[N_{\alpha p}^{(2)}\ln(x_1-\xi_1+\tau_\alpha^{(2)}(x_2-\xi_2))\\
&+\sum_{\beta=1}^{2}T_{\alpha\beta p}^{(2)}\ln(x_1-\xi_1+\tau_\alpha^{(2)}x_2-\overline{\tau}_\beta^{(2)}\xi_2)]d_{pm}^{(2)})\},
\end{aligned} \tag{22}$$

where the overhead bar denotes the complex conjugate of a complex number, $H(x)$ is the unit-step Heaviside function, the constants $Q_{\alpha\beta j}^{(p)}$ are implicitly given by

$$\begin{aligned}
N_{\gamma k}^{(2)}(A_{k\beta}^{(1)}N_{\beta p}^{(1)}+\sum_{\alpha=1}^{2}\overline{A}_{k\alpha}^{(1)}\overline{Q}_{\alpha\beta j}^{(1)}) &= Q_{\gamma\beta p}^{(2)},\\
M_{\gamma k}^{(2)}(L_{k2\beta}^{(1)}N_{\beta p}^{(1)}+\sum_{\alpha=1}^{2}\overline{L}_{k2\alpha}^{(1)}\overline{Q}_{\alpha\beta p}^{(1)}) &= Q_{\gamma\beta p}^{(2)},
\end{aligned} \tag{23}$$

and the constants $T^{(p)}_{\alpha\beta j}$ by

$$\begin{aligned} N^{(1)}_{\gamma k}(A^{(2)}_{k\beta}N^{(2)}_{\beta p} + \sum_{\alpha=1}^{2}\overline{A}^{(2)}_{k\alpha}\overline{T}^{(2)}_{\alpha\beta p}) &= T^{(1)}_{\gamma\beta p}, \\ M^{(1)}_{\gamma k}(L^{(2)}_{k2\beta}N^{(2)}_{\beta p} + \sum_{\alpha=1}^{2}\overline{L}^{(2)}_{k2\alpha}\overline{T}^{(2)}_{\alpha\beta p}) &= T^{(1)}_{\gamma\beta p}, \end{aligned} \tag{24}$$

where $\tau^{(p)}_{\alpha}$, $A^{(p)}_{k\alpha}$, $N^{(p)}_{\alpha j}$, $L^{(p)}_{kj\alpha}$, $M^{(p)}_{\gamma k}$ and $d^{(p)}_{jm}$ are respectively the constants τ_α, $A_{k\alpha}$, $N_{\alpha j}$, $L_{kj\alpha}$, $M_{\gamma k}$ and d_{jm} in Clements [7] computed using $c_{ijk\ell} = c^{(p)}_{ijk\ell}$.

From (20), the stresses $S^{(\text{perfect})}_{kjm}(x_1, x_2; \xi_1, \xi_2)$ which correspond to the displacements $\Phi^{(\text{perfect})}_{km}(x_1, x_2; \xi_1, \xi_2)$ in (22) are given by

$$\begin{aligned} & S^{(\text{perfect})}_{kjm}(x_1, x_2; \xi_1, \xi_2) \\ = \; & \frac{1}{2\pi}\,\text{Re}\{\sum_{\alpha=1}^{2}(H(x_2)H(\xi_2)L^{(1)}_{kj\alpha}[\frac{N^{(1)}_{\alpha p}}{(x_1 - \xi_1 + \tau^{(1)}_{\alpha}(x_2 - \xi_2))} \\ & + \sum_{\beta=1}^{2}\frac{Q^{(1)}_{\alpha\beta p}}{(x_1 - \xi_1 + \tau^{(1)}_{\alpha}x_2 - \overline{\tau}^{(1)}_{\beta}\xi_2)}]d^{(1)}_{pm} \\ & + H(-x_2)H(\xi_2)\sum_{\beta=1}^{2}\frac{L^{(2)}_{kj\alpha}Q^{(2)}_{\alpha\beta p}d^{(1)}_{pm}}{(x_1 - \xi_1 + \tau^{(2)}_{\alpha}x_2 - \tau^{(1)}_{\beta}\xi_2)} \\ & + H(x_2)H(-\xi_2)\sum_{\beta=1}^{2}\frac{L^{(1)}_{kj\alpha}T^{(1)}_{\alpha\beta p}d^{(2)}_{pm}}{(x_1 - \xi_1 + \tau^{(1)}_{\alpha}x_2 - \tau^{(2)}_{\beta}\xi_2)} \\ & + H(-x_2)H(-\xi_2)L^{(2)}_{kj\alpha}[\frac{N^{(2)}_{\alpha p}}{(x_1 - \xi_1 + \tau^{(2)}_{\alpha}(x_2 - \xi_2))} \\ & + \sum_{\beta=1}^{2}\frac{T^{(2)}_{\alpha\beta p}}{(x_1 - \xi_1 + \tau^{(2)}_{\alpha}x_2 - \overline{\tau}^{(2)}_{\beta}\xi_2)}]d^{(2)}_{pm})\}. \end{aligned} \tag{25}$$

3.2 Soft interface

If the interface is soft, the interface conditions for the Green's function are given by

$$\left.\begin{array}{rcl} S_{k2m}(x_1,0^+;\xi_1,\xi_2) &=& S_{k2m}(x_1,0^-;\xi_1,\xi_2) \\ S_{k2m}(x_1,0^\pm;\xi_1,\xi_2) &=& \lambda_{ks}[\Phi_{sm}(x_1,0^+;\xi_1,\xi_2)-\Phi_{sm}(x_1,0^-;\xi_1,\xi_2)] \end{array}\right\} \\ \text{for } -\infty < x_1 < \infty. \tag{26}$$

To derive $\Phi_{km} = \Phi_{km}^{(\mathrm{soft})}$ satisfying (19), (20) and (26), we take

$$\begin{aligned} \Phi_{km}^{(\mathrm{soft})}(x_1,x_2;\xi_1,\xi_2) &= \Phi_{km}^{(\mathrm{perfect})}(x_1,x_2;\xi_1,\xi_2) \\ &\quad + \mathrm{Re}\{\sum_{\alpha=1}^{2}\int_0^\infty [H(x_2)A_{k\alpha}^{(1)}E_{\alpha m}^{(1)}(p;\xi_1,\xi_2) \\ &\qquad \times \exp(ip(x_1+\tau_\alpha^{(1)}x_2)) \\ &\quad + H(-x_2)A_{k\alpha}^{(2)}E_{\alpha m}^{(2)}(p;\xi_1,\xi_2) \\ &\qquad \times \exp(-ip(x_1+\tau_\alpha^{(2)}x_2))]dp\}, \end{aligned} \tag{27}$$

and hence

$$\begin{aligned} S_{kjm}^{(\mathrm{soft})}(x_1,x_2;\xi_1,\xi_2) &= S_{kjm}^{(\mathrm{perfect})}(x_1,x_2;\xi_1,\xi_2) \\ &\quad + \mathrm{Re}\{\sum_{\alpha=1}^{2}\int_0^\infty [H(x_2)L_{kj\alpha}^{(1)}E_{\alpha m}^{(1)}(p;\xi_1,\xi_2) \\ &\qquad \times \exp(ip(x_1+\tau_\alpha^{(1)}x_2)) \\ &\quad - H(-x_2)L_{kj\alpha}^{(2)}E_{\alpha m}^{(2)}(p;\xi_1,\xi_2) \\ &\qquad \times \exp(-ip(x_1+\tau_\alpha^{(2)}x_2))]ipdp\}, \end{aligned} \tag{28}$$

where $E_{\alpha m}^{(1)}(p;\xi_1,\xi_2)$ and $E_{\alpha m}^{(2)}(p;\xi_1,\xi_2)$ are functions to be determined.

The conditions in the first line of (26) are satisfied if

$$\begin{aligned} E_{\alpha m}^{(1)}(p;\xi_1,\xi_2) &= M_{\alpha r}^{(1)}\Psi_{rm}(p;\xi_1,\xi_2), \\ E_{\alpha m}^{(2)}(p;\xi_1,\xi_2) &= M_{\alpha r}^{(2)}\overline{\Psi}_{rm}(p;\xi_1,\xi_2), \end{aligned} \tag{29}$$

where $\Psi_{rm}(p;\xi_1,\xi_2)$ are to be determined as explained below.

The conditions in the second line of (26) are rewritten as

$$\begin{aligned} & \lambda_{ks}[\Phi_{sm}^{(\mathrm{soft})}(x_1,0^+;\xi_1,\xi_2)-\Phi_{sm}^{(\mathrm{soft})}(x_1,0^-;\xi_1,\xi_2)] \\ = \;& H(\xi_2)S_{k2m}^{(\mathrm{soft})}(x_1,0^-;\xi_1,\xi_2)+H(-\xi_2)S_{k2m}^{(\mathrm{soft})}(x_1,0^+;\xi_1,\xi_2) \\ & \qquad \text{for } -\infty<x_1<\infty. \end{aligned} \tag{30}$$

If we apply the Fourier exponential transformation on both sides of (30) and use (22), (25), (27), (28) and (29) together with

$$\int_{-\infty}^{\infty}\frac{\exp(-ivx)dx}{(a-ib-x)}=H(b)2\pi i\exp(-iv(a-ib)), \tag{31}$$

where a, b and v are real numbers, we obtain

$$\begin{aligned} & \pi[\lambda_{ik}\sum_{\alpha=1}^{2}(A_{k\alpha}^{(1)}M_{\alpha r}^{(1)}-\overline{A}_{k\alpha}^{(2)}\overline{M}_{\alpha r}^{(2)})-ip\delta_{ir}]\Psi_{rm}(p;\xi_1,\xi_2) \\ = \;& -\frac{1}{2}H(\xi_2)\sum_{\alpha=1}^{2}\overline{L}_{i2\alpha}^{(2)}\sum_{\beta=1}^{2}\overline{Q}_{\alpha\beta p}^{(2)}i\exp(-ip(\xi_1+\overline{\tau}_{\beta}^{(1)}\xi_2))d_{pm}^{(1)} \\ & -\frac{1}{2}H(-\xi_2)\sum_{\alpha=1}^{2}L_{i2\alpha}^{(1)}\sum_{\beta=1}^{2}T_{\alpha\beta p}^{(1)}i\exp(-ip(\xi_1+\tau_{\beta}^{(2)}\xi_2))d_{pm}^{(2)}. \end{aligned} \tag{32}$$

Note that (31) is extracted from Erdélyi *et al.* [8].

For a fixed value of m, the functions $\Psi_{rm}(p;\xi_1,\xi_2)$ may be obtained by inverting (32) as a system of linear algebraic equations. Once $\Psi_{rm}(p;\xi_1,\xi_2)$ are determined, the integrals in (27) and (28) may be easily evaluated by using a numerical integration procedure.

Note that the Green's function for the imperfect soft interface in a less general form, that is, for the special case where $\lambda_{12}=\lambda_{21}=0$, is given in Sudak and Wang [18].

3.3 Stiff interface

If the interface is stiff, the interface conditions for the Green's function are given by

$$\left.\begin{aligned} \Phi_{km}(x_1,0^+;\xi_1,\xi_2) &= \Phi_{km}(x_1,0^-;\xi_1,\xi_2) \\ -\alpha_{kp}\frac{\partial^2\Phi_{pm}}{\partial x_1^2}\bigg|_{x_2=0^\pm} &= S_{k2m}(x_1,0^+;\xi_1,\xi_2) - S_{k2m}(x_1,0^-;\xi_1,\xi_2) \\ & \qquad \text{for } -\infty < x_1 < \infty. \end{aligned}\right\} \tag{33}$$

To derive $\Phi_{km} = \Phi_{km}^{(\text{stiff})}$ satisfying (19), (20) and (33), we take

$$\begin{aligned} \Phi_{km}^{(\text{stiff})}(x_1,x_2;\xi_1,\xi_2) &= \Phi_{km}^{(\text{perfect})}(x_1,x_2;\xi_1,\xi_2) \\ &\quad + \text{Re}\{\sum_{\alpha=1}^{2}\int_0^\infty [H(x_2)A_{k\alpha}^{(1)}F_{\alpha m}^{(1)}(p;\xi_1,\xi_2) \\ &\qquad \times \exp(ip(x_1+\tau_\alpha^{(1)}x_2)) \\ &\quad + H(-x_2)A_{k\alpha}^{(2)}F_{\alpha m}^{(2)}(p;\xi_1,\xi_2) \\ &\qquad \times \exp(-ip(x_1+\tau_\alpha^{(2)}x_2))]dp\}, \end{aligned} \tag{34}$$

and hence

$$\begin{aligned} S_{kjm}^{(\text{stiff})}(x_1,x_2;\xi_1,\xi_2) &= S_{kjm}^{(\text{perfect})}(x_1,x_2;\xi_1,\xi_2) \\ &\quad + \text{Re}\{\sum_{\alpha=1}^{2}\int_0^\infty [H(x_2)L_{kj\alpha}^{(1)}F_{\alpha m}^{(1)}(p;\xi_1,\xi_2) \\ &\qquad \times \exp(ip(x_1+\tau_\alpha^{(1)}x_2)) \\ &\quad - H(-x_2)L_{kj\alpha}^{(2)}F_{\alpha m}^{(2)}(p;\xi_1,\xi_2) \\ &\qquad \times \exp(-ip(x_1+\tau_\alpha^{(2)}x_2))]ipdp\}, \end{aligned} \tag{35}$$

where $F_{\alpha m}^{(1)}(p;\xi_1,\xi_2)$ and $F_{\alpha m}^{(2)}(p;\xi_1,\xi_2)$ are functions to be determined.

The conditions in the first line of (33) are satisfied if $F^{(1)}_{\alpha m}(p;\xi_1,\xi_2)$ and $F^{(2)}_{\alpha m}(p;\xi_1,\xi_2)$ are given by

$$\begin{aligned} F^{(1)}_{\alpha m}(p;\xi_1,\xi_2) &= N^{(1)}_{\alpha r}\Upsilon_{rm}(p;\xi_1,\xi_2), \\ F^{(2)}_{\alpha m}(p;\xi_1,\xi_2) &= N^{(2)}_{\alpha r}\overline{\Upsilon}_{rm}(p;\xi_1,\xi_2), \end{aligned} \tag{36}$$

where $\Upsilon_{rm}(p;\xi_1,\xi_2)$ are to be determined as explained below.

The conditions in the second line of (33) are rewritten as

$$\begin{aligned} & S_{k2m}(x_1,0^+;\xi_1,\xi_2) - S_{k2m}(x_1,0^-;\xi_1,\xi_2) \\ = \; & -H(\xi_2)\,\alpha_{kp}\frac{\partial^2\Phi_{pm}}{\partial x_1^2}\bigg|_{x_2=0^-} - H(-\xi_2)\,\alpha_{kp}\frac{\partial^2\Phi_{pm}}{\partial x_1^2}\bigg|_{x_2=0^+} \\ & \qquad\qquad \text{for } -\infty < x_1 < \infty. \end{aligned} \tag{37}$$

If we apply the Fourier exponential transformation on both sides of (37) and use (22), (25), (34), (35) and (36) together with (31) and

$$\int_{-\infty}^{\infty}\frac{\exp(-ivx)dx}{(a-ib-x)^2} = -H(b)2\pi v\exp(-iv(a-ib)), \tag{38}$$

where a, b and v are real numbers, we obtain

$$\begin{aligned} & \pi[i\sum_{\alpha=1}^{2}(L^{(1)}_{s2\alpha}N^{(1)}_{\alpha r} - \overline{L}^{(2)}_{s2\alpha}\overline{N}^{(2)}_{\alpha r}) - \alpha_{ir}p]\Upsilon_{rm}(p;\xi_1,\xi_2) \\ = \; & -\frac{1}{2}\alpha_{sk}H(\xi_2)\sum_{\alpha=1}^{2}\overline{A}^{(2)}_{k\alpha}\sum_{\beta=1}^{2}\overline{Q}^{(2)}_{\alpha\beta p}\exp(-ip(\xi_1+\overline{\tau}^{(1)}_{\beta}\xi_2))d^{(1)}_{pm} \\ & -\frac{1}{2}\alpha_{sk}H(-\xi_2)\sum_{\alpha=1}^{2}A^{(1)}_{k\alpha}\sum_{\beta=1}^{2}T^{(1)}_{\alpha\beta p}\exp(-ip(\xi_1+\tau^{(2)}_{\beta}\xi_2))d^{(2)}_{pm}. \end{aligned} \tag{39}$$

Note that (38) may be obtained by partially differentiating both sides of (31) with respect to either b or a.

For a fixed value of m, the functions $\Upsilon_{rm}(p;\xi_1,\xi_2)$ may be obtained by inverting (39) as a system of linear algebraic equations. Once $\Upsilon_{rm}(p;\xi_1,\xi_2)$ are determined, the integrals in (34) and (35) may be easily evaluated by using a numerical integration procedure.

4 A plane elastostatic problem

With reference to a Cartesian coordinate system $Ox_1x_2x_3$, consider an elastic body with a geometry that does not change along the x_3 axis. The body is made up of two dissimilar anisotropic materials occupying the regions $\Omega^{(1)}$ and $\Omega^{(2)}$. The interface between $\Omega^{(1)}$ and $\Omega^{(2)}$, denoted by $\mathcal{I}$, lies on part of the $x_2 = 0$ plane. A geometrical sketch of the bimaterial on the Ox_1x_2 plane is given in Figure 3. As shown in Figure 3, $C^{(1)} \cup C^{(2)}$ forms the exterior boundary of the bimaterial and the regions $\Omega^{(1)}$ and $\Omega^{(2)}$ are bounded by $\mathcal{I} \cup C^{(1)}$ and $\mathcal{I} \cup C^{(2)}$ respectively. The elastic moduli of the material in $\Omega^{(p)}$ are denoted by $c^{(p)}_{ijk\ell}$.

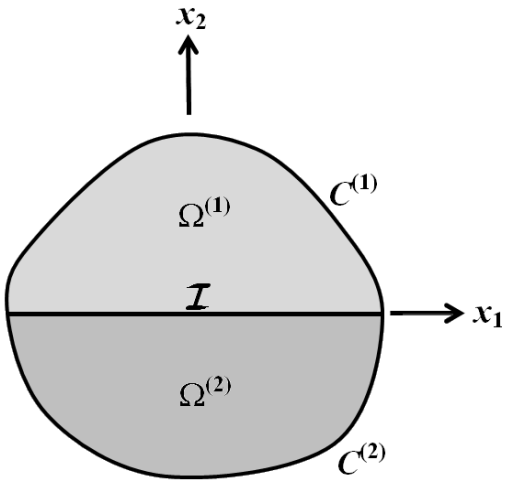

Figure 3. A sketch of the bimaterial.

Either the displacements u_k or the tractions t_k are suitably prescribed at each point on the exterior boundary $C^{(1)} \cup C^{(2)}$ of the bimaterial. The interface $\mathcal{I}$ is imperfect such that either the soft or the stiff interface conditions hold. The problem of interest is to determine the displacement and the stress

fields throughout the bimaterial $\Omega^{(1)} \cup \Omega^{(2)}$.

5 Boundary integral equations

If the interface $\mathcal{I}$ is given by $a < x_1 < b$, $x_2 = 0$, then the boundary integral equations for elastostatic deformations of the materials in $\Omega^{(1)}$ and $\Omega^{(2)}$, in the absence of body forces, are given by

$$\begin{aligned}\gamma^{(1)}(\xi_1,\xi_2)u_m(\xi_1,\xi_2) &= \int_{C^{(1)}} [u_k(x_1,x_2)\Gamma_{km}(x_1,x_2;\xi_1,\xi_2) \\ &\quad -t_k(x_1,x_2)\Phi_{km}(x_1,x_2;\xi_1,\xi_2)]ds(x_1,x_2) \\ &\quad + \int_a^b [-u_k(x_1,0^+)S_{k2m}(x_1,0^+;\xi_1,\xi_2) \\ &\quad +\sigma_{k2}(x_1,0^+)\Phi_{km}(x_1,0^+;\xi_1,\xi_2)]dx_1, \qquad (40)\end{aligned}$$

and

$$\begin{aligned}\gamma^{(2)}(\xi_1,\xi_2)u_m(\xi_1,\xi_2) &= \int_{C^{(2)}} [u_k(x_1,x_2)\Gamma_{km}(x_1,x_2;\xi_1,\xi_2) \\ &\quad -t_k(x_1,x_2)\Phi_{km}(x_1,x_2;\xi_1,\xi_2)]ds(x_1,x_2) \\ &\quad + \int_a^b [u_k(x_1,0^-)S_{k2m}(x_1,0^-;\xi_1,\xi_2) \\ &\quad -\sigma_{k2}(x_1,0^-)\Phi_{km}(x_1,0^-;\xi_1,\xi_2)]dx_1, \qquad (41)\end{aligned}$$

where Φ_{km} are any displacements satisfying the partial differential equations in (19), Γ_{km} are the tractions defined by

$$\Gamma_{km}(x_1,x_2;\xi_1,\xi_2) = S_{kjm}(x_1,x_2;\xi_1,\xi_2)n_j(x_1,x_2), \qquad (42)$$

S_{kjm} are defined in (20), $n_j(x_1,x_2)$ are components of the unit outward normal vector to $C^{(1)} \cup C^{(2)}$ at the point (x_1,x_2), and $\gamma^{(p)}(\xi_1,\xi_2)$ $(p = 1,2)$ is

defined by

$$\gamma^{(p)}(\xi_1,\xi_2)=\begin{cases}1 & \text{if } (\xi_1,\xi_2) \text{ lies in the interior of } \Omega^{(p)},\\ 1/2 & \text{if } (\xi_1,\xi_2) \text{ lies on a smooth part of } \mathcal{I}\cup C^{(p)},\\ 0 & \text{if } (\xi_1,\xi_2) \text{ lies outside } \mathcal{I}\cup C^{(p)}\cup\Omega^{(p)}.\end{cases} \tag{43}$$

Details on the derivation of the boundary integral equations in (40) and (41) may be found in Clements [7].

As we shall see below, the integration over the imperfect interface $\mathcal{I}$ in (40) and (41) may be eliminated, if Φ_{km} are chosen to be given by $\Phi_{km}^{(\text{soft})}$ and $\Phi_{km}^{(\text{stiff})}$ for soft and stiff interfaces respectively.

5.1 Soft interface

For the case where the interface is assumed to be soft, we take

$$\Phi_{km}(x_1,x_2;\xi_1,\xi_2)=\Phi_{km}^{(\text{soft})}(x_1,x_2;\xi_1,\xi_2), \tag{44}$$

where $\Phi_{km}^{(\text{soft})}$ are as given in Subsection 3.2.

If we add (40) and (41) and apply (12), (13) and (26), we obtain the boundary integral equations

$$\begin{aligned}\gamma(\xi_1,\xi_2)u_m(\xi_1,\xi_2) \;=\; & \int\limits_{C^{(1)}\cup C^{(2)}} [u_k(x_1,x_2)\Gamma_{km}^{(\text{soft})}(x_1,x_2;\xi_1,\xi_2)\\ & -t_k(x_1,x_2)\Phi_{km}^{(\text{soft})}(x_1,x_2;\xi_1,\xi_2)]ds(x_1,x_2)\\ & \text{for } (\xi_1,\xi_2)\in\Omega^{(1)}\cup\Omega^{(2)}\cup C^{(1)}\cup C^{(2)},\end{aligned} \tag{45}$$

where $\Gamma_{km}^{(\text{soft})}$ are given by

$$\Gamma_{km}^{(\text{soft})}(x_1,x_2;\xi_1,\xi_2)=S_{kjm}^{(\text{soft})}(x_1,x_2;\xi_1,\xi_2)n_j(x_1,x_2), \tag{46}$$

and $\gamma(\xi_1,\xi_2)$ by

$$\gamma(\xi_1,\xi_2)=\begin{cases}1 & \text{if } (\xi_1,\xi_2) \text{ lies in the interior of } \Omega^{(1)}\cup\Omega^{(1)},\\ 1/2 & \text{if } (\xi_1,\xi_2) \text{ lies on a smooth part of } C^{(1)}\cup C^{(2)},\\ 0 & \text{if } (\xi_1,\xi_2) \text{ lies outside the bimaterial.}\end{cases} \tag{47}$$

Note that the boundary integral equations in (45) do not contain any integral over the imperfect soft interface $\mathcal{I}$. If (45) is used to derive a boundary element procedure for solving the plane elastostatic problem stated in Section 4, only the exterior boundary $C^{(1)} \cup C^{(2)}$ of the bimaterial has to be discretized into elements.

With the use of the generalized Hooke's law, the boundary integral equations in (45) may be partially differentiated with respect to ξ_i to obtain the stress formula

$$\begin{aligned}\sigma_{ij}(\xi_1,\xi_2) &= c^{(p)}_{ijmr} \int\limits_{C^{(1)}\cup C^{(2)}} \{u_k(x_1,x_2)\frac{\partial}{\partial \xi_r}[\Gamma^{(\mathrm{soft})}_{km}(x_1,x_2;\xi_1,\xi_2)] \\ &\quad -t_k(x_1,x_2)\frac{\partial}{\partial \xi_r}[\Phi^{(\mathrm{soft})}_{km}(x_1,x_2;\xi_1,\xi_2)]\}ds(x_1,x_2) \\ &\quad \text{for } (\xi_1,\xi_2)\in\Omega^{(p)}\ (p=1,2). \end{aligned} \tag{48}$$

5.2 Stiff interface

For the case where the interface is assumed to be stiff, we take

$$\Phi_{km}(x_1,x_2;\xi_1,\xi_2) = \Phi^{(\mathrm{stiff})}_{km}(x_1,x_2;\xi_1,\xi_2), \tag{49}$$

where $\Phi^{(\mathrm{stiff})}_{km}$ are as given in Subsection 3.3.

If we add (40) and (41) and apply (15), (16) and (33), we obtain the boundary integral equations

$$\begin{aligned}\gamma(\xi_1,\xi_2)u_m(\xi_1,\xi_2) &= \int\limits_{C^{(1)}\cup C^{(2)}} [u_k(x_1,x_2)\Gamma^{(\mathrm{stiff})}_{km}(x_1,x_2;\xi_1,\xi_2) \\ &\quad -t_k(x_1,x_2)\Phi^{(\mathrm{stiff})}_{km}(x_1,x_2;\xi_1,\xi_2)]ds(x_1,x_2) \\ &\quad +\int_a^b \alpha_{kp}[u_k(x_1,0)\frac{\partial^2}{\partial x_1^2}(\Phi^{(\mathrm{stiff})}_{pm}(x_1,0;\xi_1,\xi_2)) \\ &\quad -\Phi^{(\mathrm{stiff})}_{km}(x_1,x_2;\xi_1,\xi_2)\frac{\partial^2}{\partial x_1^2}(u_p(x_1,0))]dx_1(x_1,x_2) \\ &\quad \text{for } (\xi_1,\xi_2)\in\Omega^{(1)}\cup\Omega^{(2)}\cup C^{(1)}\cup C^{(2)}, \end{aligned} \tag{50}$$

where $\Gamma_{km}^{(\text{stiff})}$ are given by

$$\Gamma_{km}^{(\text{stiff})}(x_1, x_2; \xi_1, \xi_2) = S_{kjm}^{(\text{stiff})}(x_1, x_2; \xi_1, \xi_2) n_j(x_1, x_2). \tag{51}$$

Performing integration by parts on the integral over the imperfect stiff interface, we find that (50) reduces to

$$\begin{aligned}
\gamma(\xi_1, \xi_2) u_m(\xi_1, \xi_2) \;=\; & \int\limits_{C^{(1)} \cup C^{(2)}} [u_k(x_1, x_2) \Gamma_{km}^{(\text{stiff})}(x_1, x_2; \xi_1, \xi_2) \\
& - t_k(x_1, x_2) \Phi_{km}^{(\text{stiff})}(x_1, x_2; \xi_1, \xi_2)] ds(x_1, x_2) \\
& + \alpha_{kp} \{ - u_k(a, 0) \left. \frac{\partial \Phi_{pm}^{(\text{stiff})}}{\partial x_1} \right|_{(x_1, x_2) = (a, 0)} \\
& + u_k(b, 0) \left. \frac{\partial \Phi_{pm}^{(\text{stiff})}}{\partial x_1} \right|_{(x_1, x_2) = (b, 0)} \\
& + \Phi_{km}^{(\text{stiff})}(a, 0; \xi_1, \xi_2) \left. \frac{\partial u_p}{\partial x_1} \right|_{(x_1, x_2) = (a, 0)} \\
& - \Phi_{km}^{(\text{stiff})}(b, 0; \xi_1, \xi_2) \left. \frac{\partial u_p}{\partial x_1} \right|_{(x_1, x_2) = (b, 0)} \} \\
& \text{for } (\xi_1, \xi_2) \in \Omega^{(1)} \cup \Omega^{(2)} \cup C^{(1)} \cup C^{(2)}.
\end{aligned} \tag{52}$$

Note that the boundary integral equations in (52) do not contain any integral over the stiff interface. A boundary element procedure based on (52) for solving the plane elastostatic problem in Section 4 does not require the imperfect stiff interface to be discretized into elements. Nevertheless, the values of u_k and $\partial u_k / \partial x_1$ at the interface tips $(a, 0)$ and $(b, 0)$, which appear on the right hand side of (52), must be properly treated in the boundary element procedure.

From (52), we obtain

$$\begin{aligned}\sigma_{ij}(\xi_1,\xi_2) &= c^{(p)}_{ijmr}\int\limits_{C^{(1)}\cup C^{(2)}}\{u_k(x_1,x_2)\frac{\partial}{\partial\xi_r}[\Gamma^{(\mathrm{stiff})}_{km}(x_1,x_2;\xi_1,\xi_2)]\\ &\quad -t_k(x_1,x_2)\frac{\partial}{\partial\xi_r}[\Phi^{(\mathrm{stiff})}_{km}(x_1,x_2;\xi_1,\xi_2)]\}ds(x_1,x_2)\\ &\quad +c^{(p)}_{ijmr}\alpha_{kp}\{-u_k(a,0)\left.\frac{\partial^2\Phi^{(\mathrm{stiff})}_{pm}}{\partial\xi_r\partial x_1}\right|_{(x_1,x_2)=(a,0)}\\ &\quad +u_k(b,0)\left.\frac{\partial^2\Phi^{(\mathrm{stiff})}_{pm}}{\partial\xi_r\partial x_1}\right|_{(x_1,x_2)=(b,0)}\\ &\quad +\left.\frac{\partial\Phi^{(\mathrm{stiff})}_{km}}{\partial\xi_r}\right|_{(x_1,x_2)=(a,0)}\left.\frac{\partial u_p}{\partial x_1}\right|_{(x_1,x_2)=(a,0)}\\ &\quad -\left.\frac{\partial\Phi^{(\mathrm{stiff})}_{km}}{\partial\xi_r}\right|_{(x_1,x_2)=(b,0)}\left.\frac{\partial u_p}{\partial x_1}\right|_{(x_1,x_2)=(b,0)}\}\\ &\quad \text{for } (\xi_1,\xi_2)\in\Omega^{(p)}\ (p=1,2).\end{aligned}\tag{53}$$

6 Boundary element procedures

Boundary element procedures based on (45) or (52) are proposed here for the numerical solution of the plane elastostatic problem in Section 4 for soft and stiff interfaces.

The exterior boundary $C^{(1)}\cup C^{(2)}$ of the bimaterial in Figure 3 is discretized into N straight line elements denoted by $B^{(1)}$, $B^{(2)}$, ... , $B^{(N-1)}$ and $B^{(N)}$, that is, $C^{(1)}\cup C^{(2)}$ is approximated as

$$C^{(1)}\cup C^{(2)}\simeq B^{(1)}\cup B^{(2)}\cup ...\cup B^{(N-1)}\cup B^{(N)}.\tag{54}$$

Each element is assumed to lie completely in the region given by either $x_2>0$ or $x_2<0$. The two endpoints of the elements $B^{(n)}$ are denoted by $(x_1^{(n)},x_2^{(n)})$ and $(y_1^{(n)},y_2^{(n)})$.

On $B^{(n)}$, we define the points $(\xi_1^{(n)}, \xi_2^{(n)})$ and $(\xi_1^{(N+n)}, \xi_2^{(N+n)})$ by

$$\begin{aligned}(\xi_1^{(n)}, \xi_2^{(n)}) &= (x_1^{(n)}, x_2^{(n)}) + \theta[(y_1^{(n)}, y_2^{(n)}) - (x_1^{(n)}, x_2^{(n)})], \\ (\xi_1^{(N+n)}, \xi_2^{(N+n)}) &= (x_1^{(n)}, x_2^{(n)}) + (1-\theta)[(y_1^{(n)}, y_2^{(n)}) - (x_1^{(n)}, x_2^{(n)})],\end{aligned} \tag{55}$$

where θ is a selected positive number such that $0 < \theta < 1/2$. For the numerical calculations in Section 7, we take $\theta = 1/4$.

For the displacements u_k and the tractions t_k on the elements, we make the discontinuous linear approximations

$$\left.\begin{aligned} u_k &\simeq \frac{[s^{(n)}(x_1,x_2) - (1-\theta)\ell^{(n)}]\widehat{u}_k^{(n)} - [s^{(n)}(x_1,x_2) - \theta\ell^{(n)}]\widehat{u}_k^{(N+n)}}{(2\theta-1)\ell^{(n)}} \\ t_k &\simeq \frac{[s^{(n)}(x_1,x_2) - (1-\theta)\ell^{(n)}]\widehat{t}_k^{(n)} - [s^{(n)}(x_1,x_2) - \theta\ell^{(n)}]\widehat{t}_k^{(N+n)}}{(2\theta-1)\ell^{(n)}} \end{aligned}\right\} \quad \text{for } (x_1,x_2) \in B^{(n)}, \tag{56}$$

where $\widehat{u}_k^{(p)}$ and $\widehat{t}_k^{(p)}$ are the values of u_k and t_k at the point $(\xi_1^{(p)}, \xi_2^{(p)})$ $(p = 1, 2, \cdots, 2N)$, $\ell^{(n)}$ is the length of $B^{(n)}$ and

$$s^{(n)}(x_1,x_2) = \sqrt{(x_1 - x_1^{(n)})^2 + (x_2 - x_2^{(n)})^2}. \tag{57}$$

If the displacements u_k are specified on $B^{(n)}$, then $\widehat{u}_k^{(n)}$ and $\widehat{u}_k^{(n+N)}$ are known values and $\widehat{t}_k^{(n)}$ and $\widehat{t}_k^{(n+N)}$ are unknown values to be determined. Likewise, if the tractions t_k are prescribed on $B^{(n)}$, then $\widehat{t}_k^{(n)}$ and $\widehat{t}_k^{(n+N)}$ are known values and $\widehat{u}_k^{(n)}$ and $\widehat{u}_k^{(n+N)}$ are unknown values to be determined.

6.1 Soft interface

From (54) and (56), the boundary integral equations in (45) for the soft interface may be approximated as

$$\begin{aligned}\gamma(\xi_1^{(i)},\xi_2^{(i)})\widehat{u}_m^{(i)} &= \sum_{n=1}^{N}\frac{1}{(2\theta-1)\ell^{(n)}}\\ &\times\{\widehat{u}_k^{(n)}[-(1-\theta)\ell^{(n)}G_{2km}^{(n)}(\xi_1^{(i)},\xi_2^{(i)})+G_{4km}^{(n)}(\xi_1^{(i)},\xi_2^{(i)})]\\ &+\widehat{u}_k^{(N+n)}[\theta\ell^{(n)}G_{2km}^{(n)}(\xi_1^{(i)},\xi_2^{(i)})-G_{4km}^{(n)}(\xi_1^{(i)},\xi_2^{(i)})]\\ &-\widehat{t}_k^{(n)}[-(1-\theta)\ell^{(n)}G_{1km}^{(n)}(\xi_1^{(i)},\xi_2^{(i)})+G_{3km}^{(n)}(\xi_1^{(i)},\xi_2^{(i)})]\\ &-\widehat{t}_k^{(N+n)}[\theta\ell^{(n)}G_{1km}^{(n)}(\xi_1^{(i)},\xi_2^{(i)})-G_{3km}^{(n)}(\xi_1^{(i)},\xi_2^{(i)})]\}\\ &\qquad\text{for } i=1,2,...,2N. \end{aligned}\tag{58}$$

where

$$\begin{aligned}G_{1km}^{(n)}(\xi_1,\xi_2) &= \int_{B^{(n)}}\Phi_{km}^{(\text{soft})}(x_1,x_2;\xi_1,\xi_2)ds(x_1,x_2),\\ G_{2km}^{(n)}(\xi_1,\xi_2) &= \int_{B^{(n)}}\Gamma_{km}^{(\text{soft})}(x_1,x_2;\xi_1,\xi_2)ds(x_1,x_2),\\ G_{3km}^{(n)}(\xi_1,\xi_2) &= \int_{B^{(n)}}s^{(n)}(x_1,x_2)\Phi_{km}^{(\text{soft})}(x_1,x_2;\xi_1,\xi_2)ds(x_1,x_2),\\ G_{4km}^{(n)}(\xi_1,\xi_2) &= \int_{B^{(n)}}s^{(n)}(x_1,x_2)\Gamma_{km}^{(\text{soft})}(x_1,x_2;\xi_1,\xi_2)ds(x_1,x_2).\end{aligned}\tag{59}$$

The integrals in (59) may be evaluated numerically. We may solve (58) as a system of linear algebraic equations for the unknowns values of the displacements or tractions on the boundary elements. Once the values of the displacements and tractions are known on all the elements, the displacements and the stresses at any point (ξ_1,ξ_2) in the interior of the bimaterial may be

calculated using

$$
\begin{aligned}
u_m(\xi_1,\xi_2) &= \sum_{n=1}^{N}\frac{1}{(2\theta-1)\ell^{(n)}} \\
&\quad\times\{\widehat{u}_k^{(n)}[-(1-\theta)\ell^{(n)}G_{2km}^{(n)}(\xi_1,\xi_2)+G_{4km}^{(n)}(\xi_1,\xi_2)] \\
&\quad+\widehat{u}_k^{(N+n)}[\theta\ell^{(n)}G_{2km}^{(n)}(\xi_1,\xi_2)-G_{4km}^{(n)}(\xi_1,\xi_2)] \\
&\quad-\widehat{t}_k^{(n)}[-(1-\theta)\ell^{(n)}G_{1km}^{(n)}(\xi_1,\xi_2)+G_{3km}^{(n)}(\xi_1,\xi_2)] \\
&\quad-\widehat{t}_k^{(N+n)}[\theta\ell^{(n)}G_{1km}^{(n)}(\xi_1,\xi_2)-G_{3km}^{(n)}(\xi_1,\xi_2)]\}, \qquad (60)
\end{aligned}
$$

and

$$
\begin{aligned}
&\sigma_{ij}(\xi_1,\xi_2) \\
&= \sum_{n=1}^{N}\frac{c_{ijmr}^{(p)}}{(2\theta-1)\ell^{(n)}} \\
&\quad\times\{\widehat{u}_k^{(n)}[-(1-\theta)\ell^{(n)}\frac{\partial}{\partial\xi_r}[G_{2km}^{(n)}(\xi_1,\xi_2)]+\frac{\partial}{\partial\xi_r}[G_{4km}^{(n)}(\xi_1,\xi_2)]] \\
&\quad+\widehat{u}_k^{(N+n)}[\theta\ell^{(n)}\frac{\partial}{\partial\xi_r}[G_{2km}^{(n)}(\xi_1,\xi_2)]-\frac{\partial}{\partial\xi_r}[G_{4km}^{(n)}(\xi_1,\xi_2)]] \\
&\quad-\widehat{t}_k^{(n)}[-(1-\theta)\ell^{(n)}\frac{\partial}{\partial\xi_r}[G_{1km}^{(n)}(\xi_1,\xi_2)]+\frac{\partial}{\partial\xi_r}[G_{3km}^{(n)}(\xi_1,\xi_2)]] \\
&\quad-\widehat{t}_k^{(N+n)}[\theta\ell^{(n)}\frac{\partial}{\partial\xi_r}[G_{1km}^{(n)}(\xi_1,\xi_2)]-\frac{\partial}{\partial\xi_r}[G_{3km}^{(n)}(\xi_1,\xi_2)]]\} \\
&\quad\text{for } (\xi_1,\xi_2)\in\Omega^{(p)}\ (p=1,2). \qquad (61)
\end{aligned}
$$

6.2 Stiff interface

If we proceed as before, the boundary integral equations in (52) for the stiff interface may be approximated as

$$\begin{aligned}
\gamma(\xi_1^{(i)},\xi_2^{(i)})\widehat{u}_m^{(i)} &= \sum_{n=1}^{N}\frac{1}{(2\theta-1)\ell^{(n)}} \\
&\times\{\widehat{u}_k^{(n)}[-(1-\theta)\ell^{(n)}K_{2km}^{(n)}(\xi_1^{(i)},\xi_2^{(i)})+K_{4km}^{(n)}(\xi_1^{(i)},\xi_2^{(i)})] \\
&+\widehat{u}_k^{(N+n)}[\theta\ell^{(n)}K_{2km}^{(n)}(\xi_1^{(i)},\xi_2^{(i)})-K_{4km}^{(n)}(\xi_1^{(i)},\xi_2^{(i)})] \\
&-\widehat{t}_k^{(n)}[-(1-\theta)\ell^{(n)}K_{1km}^{(n)}(\xi_1^{(i)},\xi_2^{(i)})+K_{3km}^{(n)}(\xi_1^{(i)},\xi_2^{(i)})] \\
&-\widehat{t}_k^{(N+n)}[\theta\ell^{(n)}K_{1km}^{(n)}(\xi_1^{(i)},\xi_2^{(i)})-K_{3km}^{(n)}(\xi_1^{(i)},\xi_2^{(i)})]\} \\
&+\alpha_{kp}\{-u_k(a,0)\,\frac{\partial}{\partial x_1}(\Phi_{pm}^{(\mathrm{stiff})}(x_1,x_2;\xi_1^{(i)},\xi_2^{(i)}))\Big|_{(x_1,x_2)=(a,0)} \\
&+u_k(b,0)\,\frac{\partial}{\partial x_1}(\Phi_{pm}^{(\mathrm{stiff})}(x_1,x_2;\xi_1^{(i)},\xi_2^{(i)}))\Big|_{(x_1,x_2)=(b,0)} \\
&+\Phi_{km}^{(\mathrm{stiff})}(a,0;\xi_1^{(i)},\xi_2^{(i)})\,\frac{\partial}{\partial x_1}[u_p(x_1,x_2)]\Big|_{(x_1,x_2)=(a,0)} \\
&-\Phi_{km}^{(\mathrm{stiff})}(b,0;\xi_1^{(i)},\xi_2^{(i)})\,\frac{\partial}{\partial x_1}[u_p(x_1,x_2)]\Big|_{(x_1,x_2)=(b,0)}\} \\
&\qquad\qquad \text{for } i=1,2,...,2N, \qquad (62)
\end{aligned}$$

where

$$\begin{aligned}
K_{1km}^{(n)}(\xi_1,\xi_2) &= \int_{B^{(n)}}\Phi_{km}^{(\mathrm{stiff})}(x_1,x_2;\xi_1,\xi_2)ds(x_1,x_2), \\
K_{2km}^{(n)}(\xi_1,\xi_2) &= \int_{B^{(n)}}\Gamma_{km}^{(\mathrm{stiff})}(x_1,x_2;\xi_1,\xi_2)ds(x_1,x_2), \\
K_{3km}^{(n)}(\xi_1,\xi_2) &= \int_{B^{(n)}}s^{(n)}(x_1,x_2)\Phi_{km}^{(\mathrm{stiff})}(x_1,x_2;\xi_1,\xi_2)ds(x_1,x_2), \\
K_{4km}^{(n)}(\xi_1,\xi_2) &= \int_{B^{(n)}}s^{(n)}(x_1,x_2)\Gamma_{km}^{(\mathrm{stiff})}(x_1,x_2;\xi_1,\xi_2)ds(x_1,x_2). \qquad (63)
\end{aligned}$$

In (62), the unknowns on the boundary elements are as in (58). As values of u_k and $\partial u_k/\partial x_1$ at the interface tips $(a,0)$ and $(b,0)$ are possibly unknown, more equations are needed to complement (62). The additional equations may be set up as explained below.

We assume that the interface tip $(a,0)$ is an endpoint of the first element $B^{(1)}$ and the other interface tip $(b,0)$ is an endpoint of the last element $B^{(N)}$. Furthermore, $B^{(1)}$ and $B^{(N)}$ are assumed to lie in the regions $x_2 > 0$ and $x_2 < 0$ respectively.

From the first line of (56), we obtain approximately the following formulae for the displacements at the interface tips $(a,0)$ and $(b,0)$:

$$\begin{aligned} u_k(a,0) &= \frac{[s^{(1)}(a,0)-(1-\theta)\ell^{(1)}]\widehat{u}_k^{(1)} - [s^{(1)}(a,0)-\theta\ell^{(1)}]\widehat{u}_k^{(N+1)}}{(2\theta-1)\ell^{(1)}}, \\ u_k(b,0) &= \frac{[s^{(N)}(b,0)-(1-\theta)\ell^{(N)}]\widehat{u}_k^{(N)} - [s^{(N)}(b,0)-\theta\ell^{(N)}]\widehat{u}_k^{(2N)}}{(2\theta-1)\ell^{(N)}}. \end{aligned} \tag{64}$$

For $(x_1,x_2) \in B^{(n)}$ ($n=1$ and $n=N$), if we differentiate the approximation of u_k in (56) with respect to the distance along $B^{(n)}$, we obtain

$$\begin{aligned} -n_2^{(1)} \left.\frac{\partial u_k}{\partial x_1}\right|_{(x_1,x_2)=(a,0)} + n_1^{(1)} \left.\frac{\partial u_k}{\partial x_2}\right|_{(x_1,x_2)=(a,0^+)} &= \frac{(\widehat{u}_k^{(1)} - \widehat{u}_k^{(N+1)})}{(2\theta-1)\ell^{(1)}}, \\ -n_2^{(N)} \left.\frac{\partial u_k}{\partial x_1}\right|_{(x_1,x_2)=(b,0)} + n_1^{(N)} \left.\frac{\partial u_k}{\partial x_2}\right|_{(x_1,x_2)=(b,0^-)} &= \frac{(\widehat{u}_k^{(N)} - \widehat{u}_k^{(2N)})}{(2\theta-1)\ell^{(N)}}, \end{aligned} \tag{65}$$

where $[n_1^{(k)}, n_2^{(k)}]$ is the unit outward normal vector to $B^{(k)}$.

Note that

$$\begin{aligned} \left.\frac{\partial u_k}{\partial x_1}\right|_{(x_1,x_2)=(a,0^+)} &= \left.\frac{\partial u_k}{\partial x_1}\right|_{(x_1,x_2)=(a,0^-)}, \\ \left.\frac{\partial u_k}{\partial x_1}\right|_{(x_1,x_2)=(b,0^+)} &= \left.\frac{\partial u_k}{\partial x_1}\right|_{(x_1,x_2)=(b,0^-)}, \end{aligned} \tag{66}$$

since $u_k(x_1, 0^+) = u_k(x_1, 0^-)$ for points $(x_1, 0)$ on the imperfect stiff interface.

From the generalized Hooke's law and the second line of (56), we approximately obtain

$$\begin{aligned} & c^{(1)}_{ijk1} n^{(1)}_j \left.\frac{\partial u_k}{\partial x_1}\right|_{(x_1,x_2)=(a,0)} + c^{(1)}_{ijk2} n^{(1)}_{j1} \left.\frac{\partial u_k}{\partial x_2}\right|_{(x_1,x_2)=(a,0^+)} \\ = & \frac{[s^{(1)}(a,0) - (1-\theta)\ell^{(1)}]\widehat{t}^{(1)}_k - [s^{(1)}(a,0) - \theta\ell^{(1)}]\widehat{t}^{(N+1)}_k}{(2\theta-1)\ell^{(1)}}, \\ & c^{(2)}_{ijk1} n^{(N)}_j \left.\frac{\partial u_k}{\partial x_1}\right|_{(x_1,x_2)=(b,0)} + c^{(2)}_{ijk2} n^{(N)}_{j1} \left.\frac{\partial u_k}{\partial x_2}\right|_{(x_1,x_2)=(b,0^-)} \\ = & \frac{[s^{(N)}(b,0) - (1-\theta)\ell^{(N)}]\widehat{t}^{(N)}_k - [s^{(N)}(b,0) - \theta\ell^{(N)}]\widehat{t}^{(2N)}_k}{(2\theta-1)\ell^{(N)}}. \end{aligned} \tag{67}$$

We may solve (62) together with (64), (65) and (67) for unknown values of u_k or t_k on the boundary elements and unknown values of u_k and $\partial u_k/\partial x_\ell$ at the interface tips $(a, 0)$ and $(b, 0)$. Once the unknown values are determined, the displacements and stresses at any point (ξ_1, ξ_2) in the interior of the bimaterial may be calculated using

$$\begin{aligned} u_m(\xi_1,\xi_2) = & \sum_{n=1}^{N} \frac{1}{(2\theta-1)\ell^{(n)}} \{\widehat{u}^{(n)}_k [-(1-\theta)\ell^{(n)} K^{(n)}_{2km}(\xi_1,\xi_2) + K^{(n)}_{4km}(\xi_1,\xi_2)] \\ & + \widehat{u}^{(N+n)}_k [\theta\ell^{(n)} K^{(n)}_{2km}(\xi_1,\xi_2) - K^{(n)}_{4km}(\xi_1,\xi_2)] \\ & - \widehat{t}^{(n)}_k [-(1-\theta)\ell^{(n)} K^{(n)}_{1km}(\xi_1,\xi_2) + K^{(n)}_{3km}(\xi_1,\xi_2)] \\ & - \widehat{t}^{(N+n)}_k [\theta\ell^{(n)} K^{(n)}_{1km}(\xi_1,\xi_2) - K^{(n)}_{3km}(\xi_1,\xi_2)]\} \\ & + \alpha_{kp} \{-u_k(a,0) \left.\frac{\partial}{\partial x_1}(\Phi^{(\mathrm{stiff})}_{pm}(x_1,x_2;\xi_1,\xi_2))\right|_{(x_1,x_2)=(a,0)} \\ & + u_k(b,0) \left.\frac{\partial}{\partial x_1}(\Phi^{(\mathrm{stiff})}_{pm}(x_1,x_2;\xi_1,\xi_2))\right|_{(x_1,x_2)=(b,0)} \\ & + \Phi^{(\mathrm{stiff})}_{km}(a,0;\xi_1,\xi_2) \left.\frac{\partial}{\partial x_1}[u_p(x_1,x_2)]\right|_{(x_1,x_2)=(a,0)} \\ & - \Phi^{(\mathrm{stiff})}_{km}(b,0;\xi_1,\xi_2) \left.\frac{\partial}{\partial x_1}[u_p(x_1,x_2)]\right|_{(x_1,x_2)=(b,0)} \}, \end{aligned} \tag{68}$$

and

$$
\begin{aligned}
&\sigma_{ij}(\xi_1,\xi_2)\\
=\ &\sum_{n=1}^{N}\frac{c^{(p)}_{ijmr}}{(2\theta-1)\ell^{(n)}}\\
&\times\{\widehat{u}^{(n)}_k[-(1-\theta)\ell^{(n)}\frac{\partial}{\partial\xi_r}[K^{(n)}_{2km}(\xi_1,\xi_2)]+\frac{\partial}{\partial\xi_r}[K^{(n)}_{4km}(\xi_1,\xi_2)]]\\
&+\widehat{u}^{(N+n)}_k[\theta\ell^{(n)}\frac{\partial}{\partial\xi_r}[K^{(n)}_{2km}(\xi_1,\xi_2)]-\frac{\partial}{\partial\xi_r}[K^{(n)}_{4km}(\xi_1,\xi_2)]]\\
&-\widehat{t}^{(n)}_k[-(1-\theta)\ell^{(n)}\frac{\partial}{\partial\xi_r}[K^{(n)}_{1km}(\xi_1,\xi_2)]+\frac{\partial}{\partial\xi_r}[K^{(n)}_{3km}(\xi_1,\xi_2)]]\\
&-\widehat{t}^{(N+n)}_k[\theta\ell^{(n)}\frac{\partial}{\partial\xi_r}[K^{(n)}_{1km}(\xi_1,\xi_2)]-\frac{\partial}{\partial\xi_r}[K^{(n)}_{3km}(\xi_1,\xi_2)]]\}\\
&+c^{(p)}_{ijmr}\alpha_{kp}\{-u_k(a,0)\left.\frac{\partial^2\Phi^{(\mathrm{stiff})}_{pm}}{\partial\xi_r\partial x_1}\right|_{(x_1,x_2)=(a,0)}\\
&+u_k(b,0)\left.\frac{\partial^2\Phi^{(\mathrm{stiff})}_{pm}}{\partial\xi_r\partial x_1}\right|_{(x_1,x_2)=(b,0)}\\
&+\left.\frac{\partial\Phi^{(\mathrm{stiff})}_{km}}{\partial\xi_r}\right|_{(x_1,x_2)=(a,0)}\left.\frac{\partial}{\partial x_1}[u_p(x_1,x_2)]\right|_{(x_1,x_2)=(a,0)}\\
&-\left.\frac{\partial\Phi^{(\mathrm{stiff})}_{km}}{\partial\xi_r}\right|_{(x_1,x_2)=(b,0)}\left.\frac{\partial}{\partial x_1}[u_p(x_1,x_2)]\right|_{(x_1,x_2)=(b,0)}\}\\
&\text{for } (\xi_1,\xi_2)\in\Omega^{(p)}\ (p=1,2).
\end{aligned}
\tag{69}
$$

7 Numerical results for particular cases

Consider the rectangular bilayered slab in Figure 4. The vertices of the rectangular slab are (w,h), $(w,-h)$, $(-w,-h)$ and $(-w,h)$, where w and h are given positive real numbers. The regions $\Omega^{(1)}$ and $\Omega^{(2)}$ are occupied by particular transversely isotropic materials. Specifically, the only non-zero

elastic moduli $c^{(p)}_{ijk\ell}$ in $\Omega^{(p)}$ are given by

$$\begin{aligned} c^{(p)}_{1111} &= C^{(p)},\ c^{(p)}_{2222} = A^{(p)}, \\ c^{(p)}_{1212} &= c^{(p)}_{2112} = c^{(p)}_{1221} = c^{(p)}_{2121} = L^{(p)}, \\ c^{(p)}_{1122} &= c^{(p)}_{2211} = F^{(p)}, \end{aligned} \tag{70}$$

where $A^{(p)}$, $F^{(p)}$, $C^{(p)}$ and $L^{(p)}$ are independent elastic coefficients.

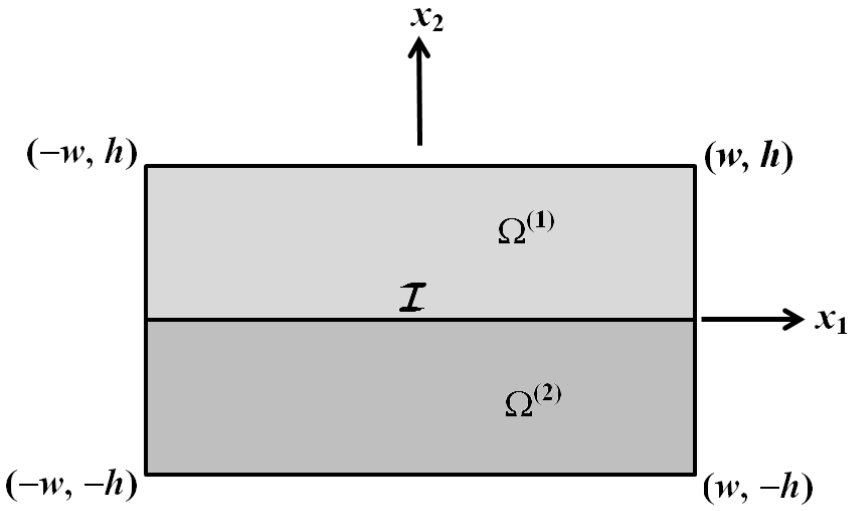

Figure 4. A rectangular bilayered slab.

The boundary conditions on the exterior boundary of the rectangular slab are given by

$$\left.\begin{aligned} u_k(x_1, -h) &= 0 \\ \sigma_{k2}(x_1,\ h) &= P_k(x_1) \end{aligned}\right\} \text{ for } -w < x_1 < w,$$
$$\sigma_{k1}(\pm w, x_2) = 0 \text{ for } -h < x_2 < h, \tag{71}$$

where $P_k(x_1)$ are suitably prescribed tractions.

The interface between the materials in $\Omega^{(1)}$ and $\Omega^{(2)}$ is imperfect, satisfying either the soft or stiff interface conditions.

Problem 1. For the mere purpose of checking the validity of the boundary element procedures, that is, for a test problem, we take $h = 0.5$, $w = 8$, $P_k(x_1) = \exp(-|x_1|)$, $A^{(1)} = 5$, $C^{(1)} = 4$, $F^{(1)} = 1$, $L^{(1)} = 1$, $A^{(2)} = 1$, $C^{(2)} = 1$, $F^{(2)} = 1/2$ and $L^{(2)} = 1/5$.

The exterior boundary of the bimaterial is discretized into 132 boundary elements and the boundary element method together with the relevant Green's function is used to compute the displacements $u_k(x_1, 0.25)$ $(-8 < x_1 < 8)$ and $u_k(0.5, x_2)$ $(-0.5 < x_2 < 0.5)$ for soft and stiff interfaces. For the parameters in the interface conditions, we take $\lambda_{11} = 2$, $\lambda_{12} = \lambda_{21} = 0$ and $\lambda_{22} = 5$ for the soft interface and $\alpha_{11} = 1/10$ and $\alpha_{12} = \alpha_{21} = \alpha_{22} = 0$ for the stiff interface.

As the width $2w$ of the rectangular slab is relatively large compared to the height $2h$, that is, $w/h = 16$, we compare the computed displacements with the corresponding explicit solutions for an infinitely long slab where $w \to \infty$. The explicit solutions are derived analytically in the Appendix − they are expressed in terms of Fourier integrals which may be evaluated numerically.

For the soft interface, Figures 5 and 6 compare graphically the values of the displacements $u_k(x_1, 0.25)$ (for $-8 < x_1 < 8$) computed using the Green's function boundary element method and those calculated using the explicit analytical solution in the Appendix. On the whole, the two sets of value agree well. Observing more closely, we find that the displacements computed using the boundary element method actually deviate slightly from the analytical solution at both ends of the slab in Figure 4. This is to be expected since the analytical solution is derived using for an infinitely long slab instead of the finite width slab in Figure 4.

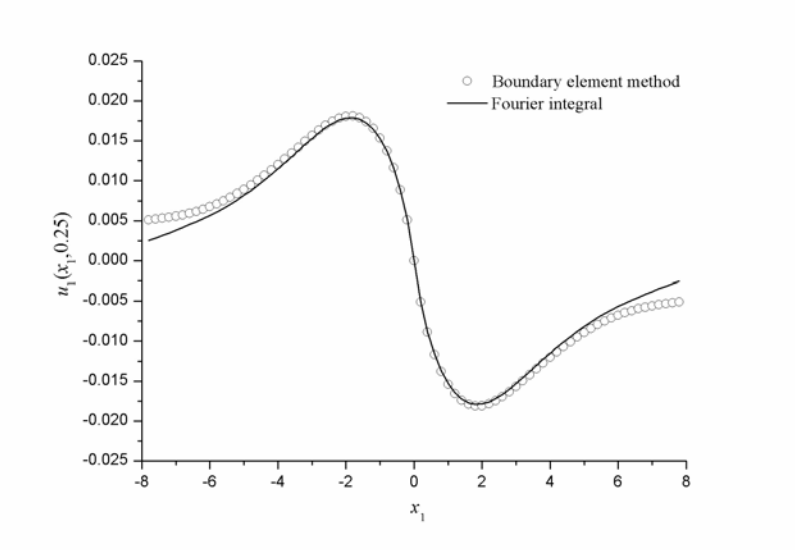

Figure 5. Plots of $u_1(x_1, 0.25)$ against x_1 for $-8 < x_1 < 8$.

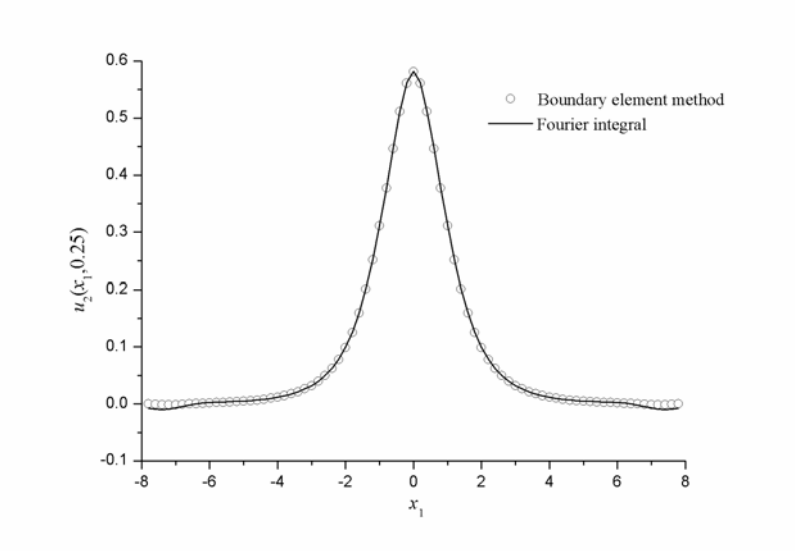

Figure 6. Plots of $u_2(x_1, 0.25)$ against x_1 for $-8 < x_1 < 8$.

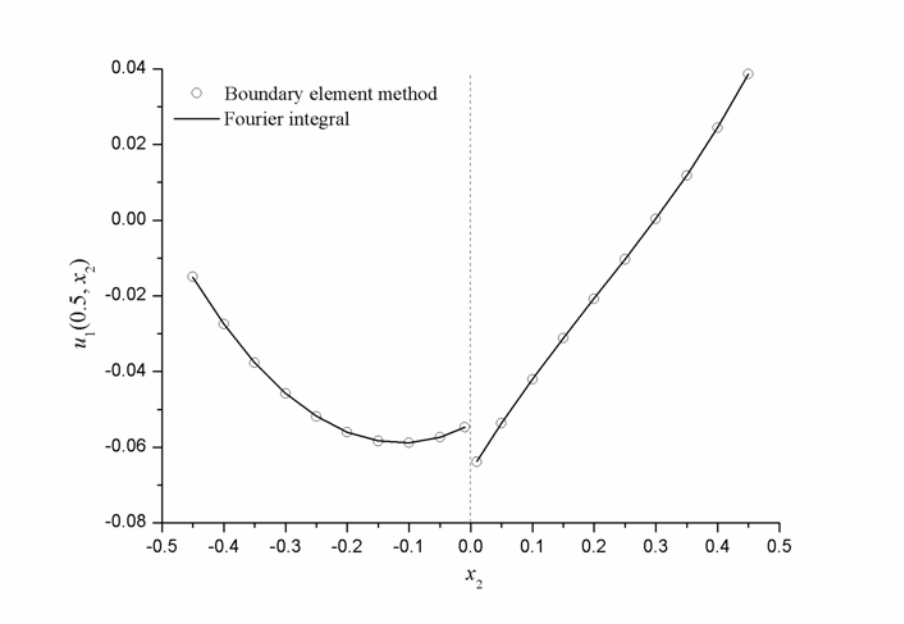

Figure 7. Plots of $u_1(0.5, x_2)$ against x_2 for $-0.5 < x_2 < 0.5$.

Plots of the displacements $u_k(0.5, x_2)$ along the direction perpendicular to the interface I are given in Figures 7 and 8 for $-0.5 < x_2 < 0.5$. Again, the values computed using the boundary element method match well the values calculated using the analytical solution. Figures 7 and 8 show clearly the displacement jumps $\triangle u_k$ across the soft interface $\mathcal{I}$.

For the stiff interface, we have also observed a good agreement between the boundary element and the analytical solutions for the displacements $u_k(x_1, 0.25)$ $(-8 < x_1 < 8)$ in Figures 9 and 10. The slight differences between the solutions at points closer to $x_1 = \pm 8$ are as explained above for the soft interface. Figures 11 and 12 show the displacements along $(0.5, x_2)$ for $-0.5 < x_2 < 0.5$ for both numerical and analytical model. As expected, we observe continuity of displacements u_k across the stiff interface $\mathcal{I}$.

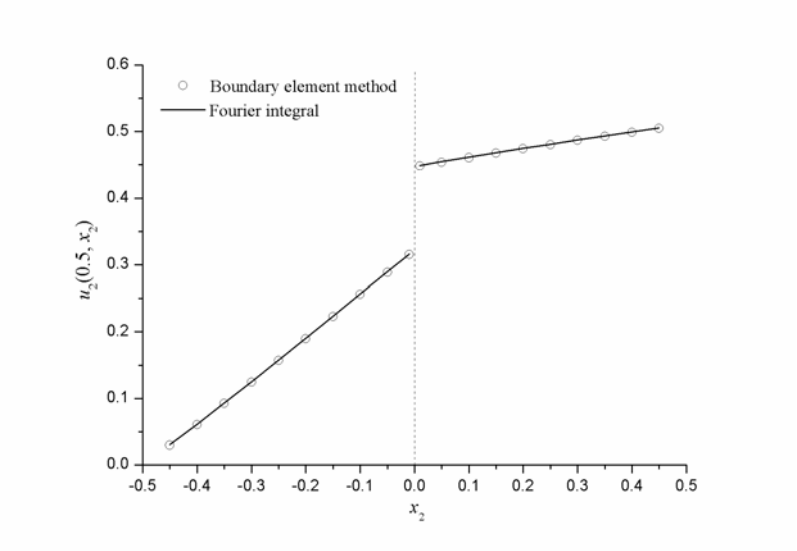

Figure 8. Plots of $u_2(0.5, x_2)$ against x_2 for $-0.5 < x_2 < 0.5$.

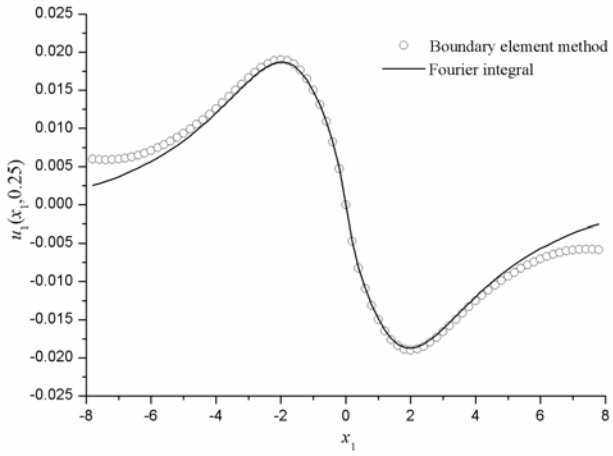

Figure 9. Plots of $u_1(x_1, 0.25)$ against x_1 for $-8 < x_1 < 8$.

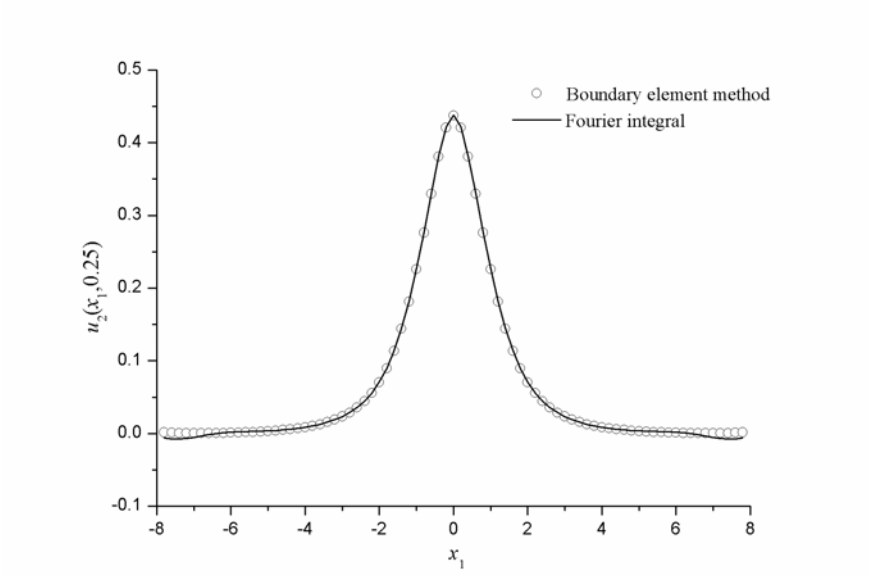

Figure 10. Plots of $u_2(x_1, 0.25)$ against x_1 for $-8 < x_1 < 8$.

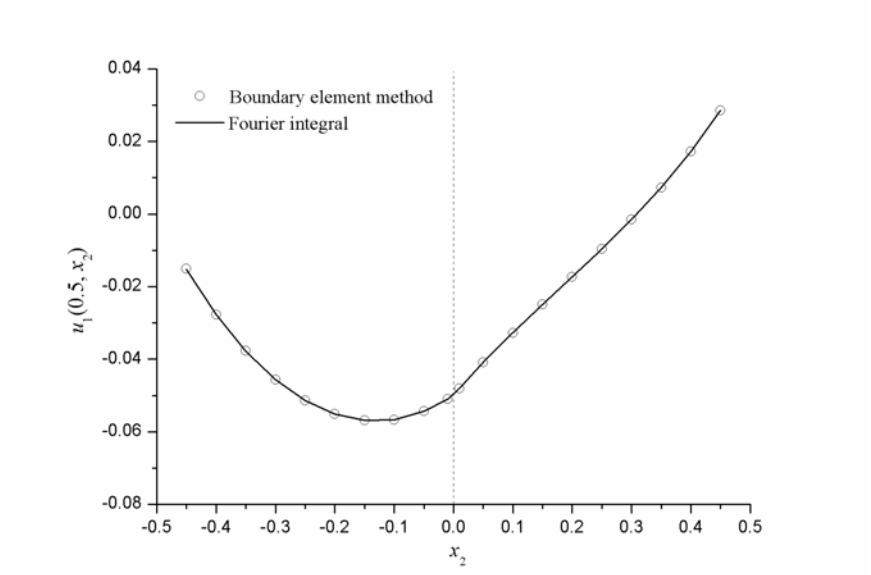

Figure 11. Plots of $u_1(0.5, x_2)$ against x_2 for $-0.5 < x_2 < 0.5$.

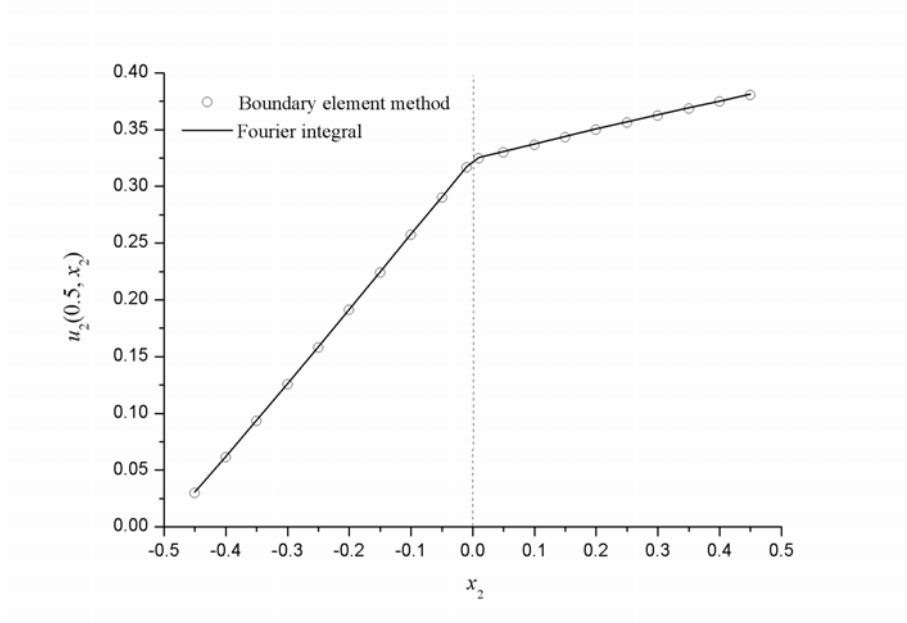

Figure 12. Plots of $u_2(0.5, x_2)$ against x_2 for $-0.5 < x_2 < 0.5$.

Table 1. Boundary element and analytical values of the stresses in the bimaterial with the soft interface.

Point	Boundary Element Method			Analytical		
(x_1, x_2)	σ_{11}	σ_{12}	σ_{22}	σ_{11}	σ_{12}	σ_{22}
$(-0.60, -0.25)$	0.0675	0.1094	0.5656	0.0679	0.1093	0.5667
$(-1.00, 0.20)$	0.0613	0.057	0.3957	0.0616	0.0576	0.3966
$(4.00, -0.40)$	0.0115	-0.0078	0.0187	0.0115	-0.0076	0.0187
$(2.00, -0.20)$	0.0968	-0.0218	0.1417	0.0971	-0.0218	0.1420
$(2.50, -0.40)$	0.0514	-0.0259	0.0843	0.0515	-0.0259	0.0844

At selected points in the interior of the bimaterial, the stresses σ_{ij} computed using (61) (for the soft interface) and (69) (for the stiff interface) are

compared in respectively Tables 1 and 2 with the values from the analytical solutions in the Appendix. It is obvious that there is a good agreement between the boundary element and the analytical values of the stresses.

Table 2. Boundary element and analytical values of the stresses in the bimaterial with the stiff interface.

Point	Boundary Element Method			Analytical		
(x_1, x_2)	σ_{11}	σ_{12}	σ_{22}	σ_{11}	σ_{12}	σ_{22}
$(-0.60, -0.25)$	0.0656	0.0930	0.5648	0.0676	0.0929	0.5657
$(-1.00, 0.20)$	0.0547	0.0500	0.3933	0.0539	0.0469	0.3926
$(4.00, -0.40)$	0.0110	-0.0077	0.0193	0.0115	-0.0080	0.0189
$(2.00, -0.20)$	0.0936	-0.0196	0.1391	0.0934	-0.0193	0.1393
$(2.50, -0.40)$	0.0496	-0.0245	0.0830	0.0500	-0.0244	0.0830

Problem 2. Consider now the case where $\Omega^{(1)}$ and $\Omega^{(2)}$ are occupied by isotropic materials. The Young's modulus and the Poisson ratio of the isotropic material in $\Omega^{(p)}$ $(p = 1, 2)$ are denoted by $E^{(p)}$ and $\nu^{(p)}$ respectively. The boundary element analysis here may be recovered for isotropic materials by taking the constants $A^{(p)}$, $F^{(p)}$, $C^{(p)}$ and $L^{(p)}$ in (70) to be approximately given by

$$\begin{aligned} A^{(p)} &= C^{(p)} = \frac{E^{(p)}(1-\nu^{(p)})}{(1+\nu^{(p)})(1-2\nu^{(p)})}, \\ F^{(p)} &= \frac{E^{(p)}\nu^{(p)}(1-\epsilon)}{(1+\nu^{(p)})(1-2\nu^{(p)})}, \; L^{(p)} = \frac{E^{(p)}}{2(1+\nu^{(p)})}, \end{aligned}$$

where ϵ is a positive real number with a very small magnitude.

The boundary conditions are as given in (71) with

$$P_k(x_1) = \begin{cases} \delta_{k2}T & \text{for } |x_1| < a, \\ 0 & \text{for } a < |x_1| < w, \end{cases}$$

where T is a given positive real constant and a is a given positive real number such that $a < w$.

For the purpose of our calculation here, we take $w/h = 2$, $a/h = 1$, $\epsilon = 10^{-6}$, $\nu^{(1)} = \nu^{(2)} = 0.30$ and $E^{(1)}/E^{(2)} = 2$ (the material in $\Omega^{(2)}$ is "softer" than that in $\Omega^{(1)}$). The exterior boundary $C_1 \cup C_2$ of the rectangular slab is discretized into 60 elements.

For the case where the interface is soft, we take $\lambda_{11}/\lambda_{22} = 0.2$, $\lambda_{12}h/E^{(1)} = \lambda_{21}h/E^{(1)} = 0$ and examine the effects of altering the parameter $\lambda_{11}h/E^{(1)}$ on the deformation of the rectangular slab. Plots of the non-dimensionalized displacements $u_k E^{(1)}/hT$ along $x_2/h = 0.5$ for $-2 < x_1/h < 2$ are given in Figures 13 and 14 for selected values of $\lambda_{11}h/E^{(1)}$. The solid line plots in both figures give the non-dimensionalized displacements $u_k E^{(1)}/hT$ for the case in which the interface is perfectly bonded, that is, for the limiting case where $\lambda_{11}h/E^{(1)} \to \infty$. In Figures 13 and 14, $u_1 E^{(1)}/hT$ approaches the solid line as the non-dimensionalized parameter $\lambda_{11}h/E^{(1)}$ increases. Hence, a lower value of $\lambda_{11}h/E^{(1)}$ indicates a weaker interface. This may also be seen in the plots of the displacement $u_2 E^{(1)}/hT$ along $x_1/h = 0$ for $-1 < x_2/h < 1$ in Figure 15, where we observe a larger deformation for a smaller value of $\lambda_{11}h/E^{(1)}$. A weaker interface is less able to distribute out the stress in $\Omega^{(1)}$ to $\Omega^{(2)}$ across the interface. As may be expected, Figure 15 shows that a smaller value of $\lambda_{11}h/E^{(1)}$ gives a bigger jump in the displacement $u_2 E^{(1)}/hT$ across the interface $\mathcal{I}$. Note that the displacement $u_2 E^{(1)}/hT$ in Figure 15 does not show any jump across the ideal interface.

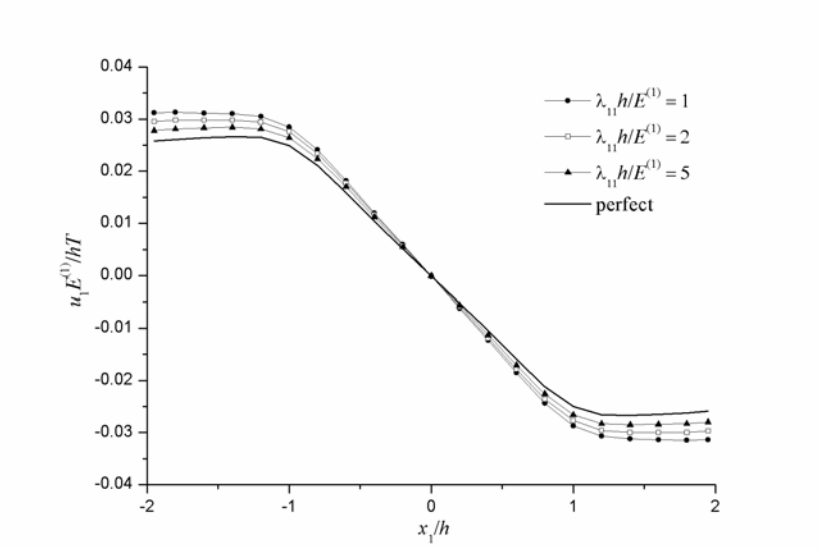

Figure 13. Plots of $u_1E^{(1)}/hT$ on $x_2/h = 0.5$, $-2 < x_1/h < 2$, for selected values of $\lambda_{11}h/E^{(1)}$.

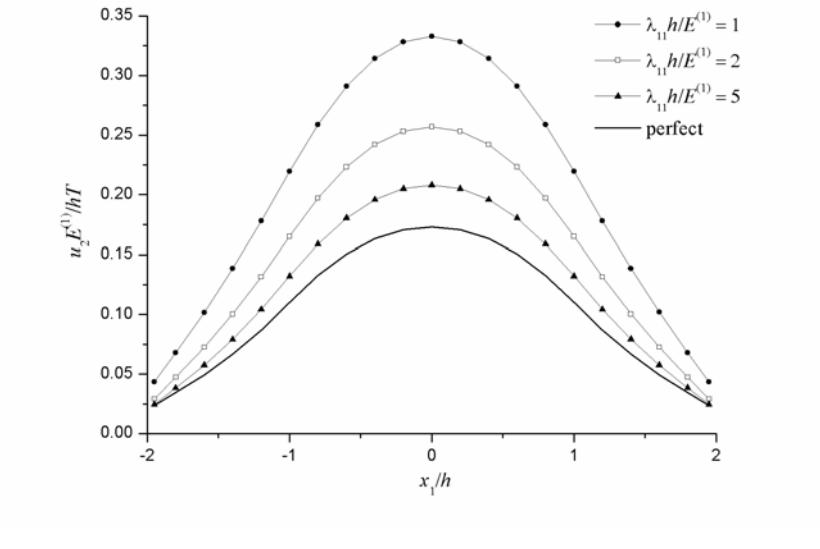

Figure 14. Plots of $u_2E^{(1)}/hT$ on $x_2/h = 0.5$, $-2 < x_1/h < 2$, for selected values of $\lambda_{11}h/E^{(1)}$.

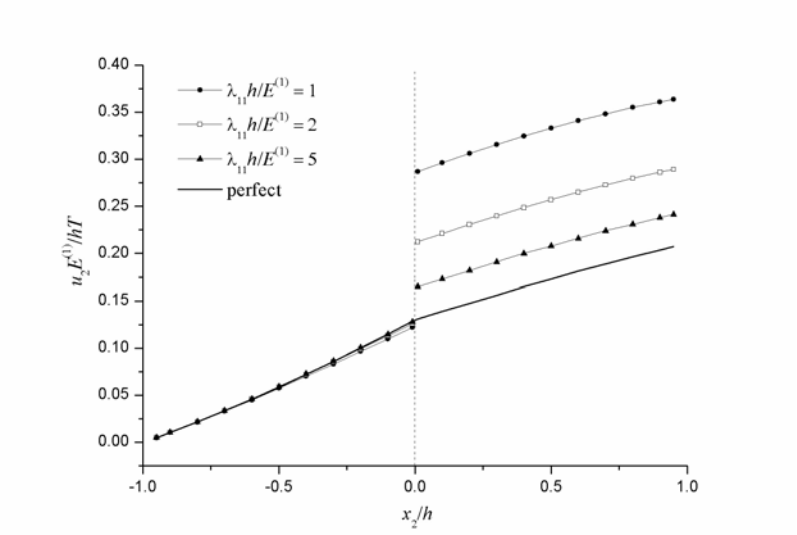

Figure 15. Plots of $u_2E^{(1)}/hT$ along $x_1/h = 0$, $-1 < x_2/h < 1$, for selected values of $\lambda_{11}h/E^{(1)}$.

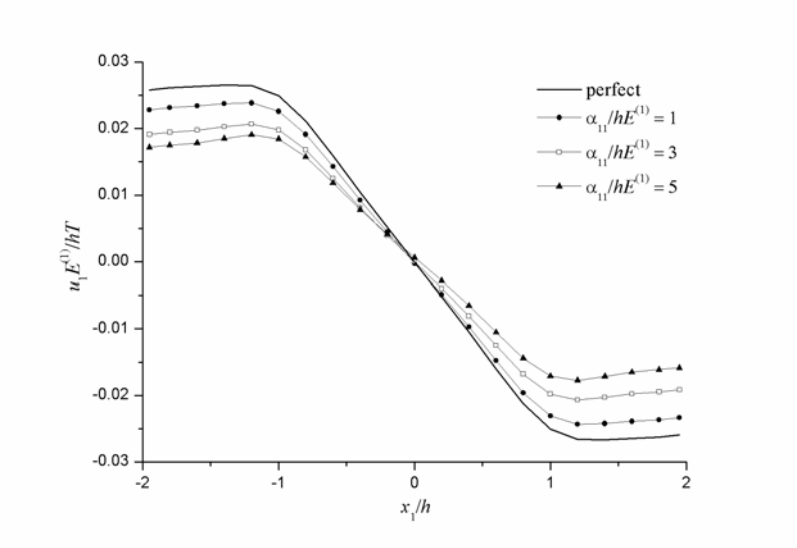

Figure 16. Plots of $u_1E^{(1)}/hT$ on $x_2/h = 0.5$, $-2 < x_1/h < 2$, for selected values of $\alpha_{11}/E^{(1)}h$.

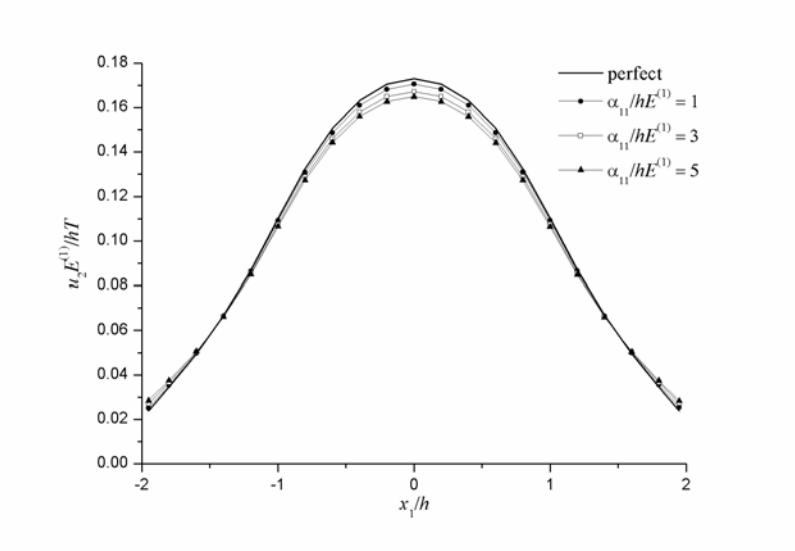

Figure 17. Plots of $u_2E^{(1)}/hT$ on $x_2/h = 0.5$, $-2 < x_1/h < 2$, for selected values of $\alpha_{11}/E^{(1)}h$.

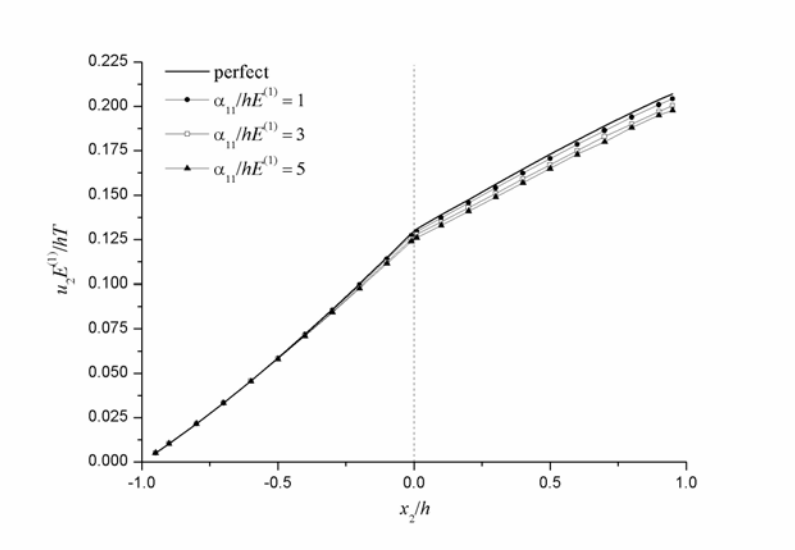

Figure 18. Plots of $u_2E^{(1)}/hT$ along $x_1/h = 0$, $-1 < x_2/h < 1$, for selected values of $\alpha_{11}/E^{(1)}h$.

For the case where the interface is stiff, we take α_{ij} to be such that only α_{11} is not zero. Figures 16, 17 and 18 show plots of the non-dimensionalized displacements $u_k E^{(1)}/hT$ for selected values of $\alpha_{11}/E^{(1)}h$. As before, the solid line plots give the non-dimensionalized displacements $u_k E^{(1)}/hT$ for the special case where the interface is ideal.

We observe that the effect of the stiff interface on the displacement field is opposite to that of the soft interface. The presence of the stiff interface appears to reduce the magnitudes of the displacements. In Figure 16, the displacement $u_1 E^{(1)}/hT$ approaches the solid line as $\alpha_{11}/E^{(1)}h$ decreases, that is, as the stiffness of the interface decreases. Figures 17 and 18 also show that the stiff interface is able to resist deformation. Moreover, in Figure 18, the gradient of the non-dimensionalized displacement $u_2 E^{(1)}/hT$ appears to decrease as non-dimensionalized stiff interface parameter $\alpha_{11}/E^{(1)}h$ increases, that is, the overall strength of the bimaterial apparently increases with increasing $\alpha_{11}/E^{(1)}h$. As expected, the displacement $u_2 E^{(1)}/hT$ is continuous across the stiff interface.

8 Summary

Green's functions are derived for imperfect soft and stiff planar interfaces between two dissimilar anisotropic elastic half spaces and applied to obtain boundary element procedures for determining the elastic fields in bimaterials of finite extent. As the derived Green's functions satisfy the relevant interface conditions, the boundary element formulations do not require the interfaces to be discretized into elements, giving rise to smaller systems of linear algebraic equations.

To access the validity and accuracy of the proposed boundary element

methods for the bimaterials with soft and stiff interfaces, specific test problems involving a relatively long rectangular bilayered slabs are solved numerically. The boundary element solutions obtained compare favorably with the analytical solutions for the corresponding case of an infinitely long bilayered slab. The boundary element procedures are also applied to study the effects of interface parameters on the displacement fields in bilayered slabs with soft and stiff interfaces. The bilayered slabs are shown to be weakened by soft interfaces and strengthened by stiff interfaces.

Appendix

The displacements and stresses in the rectangular bilayered slab in Figure 4, which satisfy the exterior boundary conditions (71) and the imperfect interface conditions, are given here explicitly in terms of Fourier integrals for the special case where $w \to \infty$, that is, for an infinitely long bilayered slab.

Guided by the analysis in Clements [7], we take the displacements to be in the form

$$\begin{aligned} & u_k(x_1, x_2) \\ = \; & H(x_2)\,\mathrm{Re}\{\sum_{\alpha=1}^{2} A_{k\alpha}^{(1)} \int_0^\infty [V_\alpha^{(1)}(p)\exp(ip(x_1+\tau_\alpha^{(1)}x_2)) \\ & + W_\alpha^{(1)}(p)\exp(-ip(x_1+\tau_\alpha^{(1)}x_2))]dp\} \\ & + H(-x_2)\,\mathrm{Re}\{\sum_{\alpha=1}^{2} A_{k\alpha}^{(2)} \int_0^\infty [V_\alpha^{(2)}(p)\exp(ip(x_1+\tau_\alpha^{(2)}x_2)) \\ & + W_\alpha^{(2)}(p)\exp(-ip(x_1+\tau_\alpha^{(2)}x_2))]dp\}, \end{aligned} \tag{A1}$$

where $V_\alpha^{(k)}(p)$ and $W_\alpha^{(k)}(p)$ $(k = 1, 2)$ are functions yet to be determined.

The stresses corresponding to the displacements in (A1) are given by

$$\begin{aligned}
&\sigma_{kj}(x_1, x_2) \\
= \;& H(x_2)\,\mathrm{Re}\{\sum_{\alpha=1}^{2} L_{kj\alpha}^{(1)} \int_0^\infty [ipV_\alpha^{(1)}(p)\exp(ip(x_1+\tau_\alpha^{(1)}x_2)) \\
& -ipW_\alpha^{(1)}(p)\exp(-ip(x_1+\tau_\alpha^{(1)}x_2))]dp\} \\
& +H(-x_2)\,\mathrm{Re}\{\sum_{\alpha=1}^{2} L_{kj\alpha}^{(2)} \int_0^\infty [ipV_\alpha^{(2)}(p)\exp(ip(x_1+\tau_\alpha^{(2)}x_2)) \\
& -ipW_\alpha^{(2)}(p)\exp(-ip(x_1+\tau_\alpha^{(2)}x_2))]dp\}. \qquad \text{(A2)}
\end{aligned}$$

If the integrals in (A2) exist, the stresses σ_{kj} decay to zero as $|x_1|$ tends to infinity (Sneddon [16]).

From (A1), we find that the conditions on the lower edge $x_2 = -h$ of the infinitely long slab, that is,

$$u_k(x_1, -h) = 0 \text{ for } -\infty < x_1 < \infty, \qquad \text{(A3)}$$

are satisfied if $V_\alpha^{(2)}(p)$ and $W_\alpha^{(2)}(p)$ are such that

$$\sum_{\alpha=1}^{2}[A_{k\alpha}^{(2)}V_\alpha^{(2)}(p)\exp(-ip\tau_\alpha^{(2)}h) + \overline{A}_{k\alpha}^{(2)}\overline{W}_\alpha^{(2)}(p)\exp(-ip\overline{\tau}_\alpha^{(2)}h)] = 0. \qquad \text{(A4)}$$

The conditions on the upper edge $x_2 = h$ of the infinitely long slab are given by

$$\sigma_{k2}(x_1, h) = P_k(x_1) \text{ for } -\infty < x_1 < \infty. \qquad \text{(A5)}$$

If we apply the Fourier exponential transformation on both sides of (A5), that is, if we rewrite (A5) as

$$\int_{-\infty}^{\infty} \sigma_{k2}(x_1, h)\exp(-i\gamma x_1)dx_1 = \int_{-\infty}^{\infty} P_k(x_1)\exp(-i\gamma x_1)dx_1, \qquad \text{(A6)}$$

and use (A2), we obtain

$$\pi ip \sum_{\alpha=1}^{2} [L_{k2\alpha}^{(1)} V_{\alpha}^{(1)}(p) \exp(ip\tau_{\alpha}^{(1)} h) + \overline{L}_{k2\alpha}^{(1)} \overline{W}_{\alpha}^{(1)}(p) \exp(ip\overline{\tau}_{\alpha}^{(1)} h)]$$
$$= \int_{-\infty}^{\infty} P_k(x_1) \exp(-ipx_1) dx_1. \tag{A7}$$

A.1 Soft interface

The conditions in (12) are satisfied if

$$\sum_{\alpha=1}^{2} [L_{i2\alpha}^{(1)} V_{\alpha}^{(1)}(p) + \overline{L}_{i2\alpha}^{(1)} \overline{W}_{\alpha}^{(1)}(p)] = \sum_{\alpha=1}^{2} [L_{i2\alpha}^{(2)} V_{\alpha}^{(2)}(p) + \overline{L}_{i2\alpha}^{(2)} \overline{W}_{\alpha}^{(2)}(p)]. \tag{A8}$$

The conditions in (13) give

$$\lambda_{ik} \{ \sum_{\alpha=1}^{2} [A_{k\alpha}^{(1)} V_{\alpha}^{(1)}(p) - A_{k\alpha}^{(2)} V_{\alpha}^{(2)}(p) + \overline{A}_{k\alpha}^{(1)} \overline{W}_{\alpha}^{(1)}(p) - \overline{A}_{k\alpha}^{(2)} \overline{W}_{\alpha}^{(2)}(p)] \}$$
$$= ip \sum_{\alpha=1}^{2} [L_{i2\alpha}^{(1)} V_{\alpha}^{(1)}(p) + \overline{L}_{i2\alpha}^{(1)} \overline{W}_{\alpha}^{(1)}(p)]. \tag{A9}$$

Thus, if the interface $\mathcal{I}$ is soft, the functions $V_{\alpha}^{(1)}$, $W_{\alpha}^{(1)}(p)$, $V_{\alpha}^{(2)}(p)$, and $W_{\alpha}^{(2)}(p)$ are obtained by solving (A4), (A7), (A8) and (A9).

A.2 Stiff interface

The conditions in (15) hold if

$$\sum_{\alpha=1}^{2} [A_{k\alpha}^{(1)} V_{\alpha}^{(1)}(p) + \overline{A}_{k\alpha}^{(1)} \overline{W}_{\alpha}^{(1)}(p)] = \sum_{\alpha=1}^{2} [A_{k\alpha}^{(2)} V_{\alpha}^{(2)}(p) + \overline{A}_{k\alpha}^{(2)} \overline{W}_{\alpha}^{(2)}(p)]. \tag{A10}$$

The conditions in (16) are satisfied if

$$i \{ \sum_{\alpha=1}^{2} [L_{i2\alpha}^{(1)} V_{\alpha}^{(1)}(p) + \overline{L}_{i2\alpha}^{(1)} \overline{W}_{\alpha}^{(1)}(p) - L_{i2\alpha}^{(2)} V_{\alpha}^{(2)}(p) - \overline{L}_{i2\alpha}^{(2)} \overline{W}_{\alpha}^{(2)}(p)] \}$$
$$= p\alpha_{ik} \sum_{\alpha=1}^{2} [A_{k\alpha}^{(1)} V_{\alpha}^{(1)}(p) + \overline{A}_{k\alpha}^{(1)} \overline{W}_{\alpha}^{(1)}(p)]. \tag{A11}$$

Thus, if the interface $\mathcal{I}$ is stiff, the functions $V_\alpha^{(1)}$, $W_\alpha^{(1)}(p)$, $V_\alpha^{(2)}(p)$, and $W_\alpha^{(2)}(p)$ are obtained by solving (A4), (A7), (A10) and (A11).

References

[1] J. D. Achenbach and H. Zhu, Effect of interfacial zone on mechanical behavior and failure of fiber-reinforced composites, *Journal of the Mechanical and Physics of Solids* **37** (1989) 381-393.

[2] W. T. Ang and Y. S. Park, Hypersingular integral equations for arbitrarily located planar cracks in an anisotropic bimaterial, *Engineering Analysis with Boundary Elements* **20** (1997) 135-143.

[3] M. Abramowitz and I. Stegun, *Handbook of Mathematical Functions*, Dover, New York, 1970.

[4] Y. Benveniste and T. Miloh, Imperfect soft and stiff interfaces in two-dimensional elasticity, *Mechanics of Materials* **33** (2001) 309-323.

[5] J. R. Berger and V. K. Tewary, Elastic Green's function for a damaged interface in anisotropic materials, *Journal of Materials Research* **11** (1996) 537-544.

[6] J. R. Berger and V. K. Tewary, Green's functions for boundary element analysis of anisotropic bimaterials, *Engineering Analysis with Boundary Elements* **25** (2001) 279-288.

[7] DL Clements, *Boundary Value Problems Governed by Second Order Elliptic Systems*, Pitman, London, 1981.

[8] A. Erdélyi, M. Magnus, F. Oberhettinger and F. Tricomi, *Tables of Integral Transforms − Volume 1*, MacGraw-Hill, New York, 1954.

[9] H. Fan and G. F. Wang, Screw dislocation interacting with an imperfect interface, *Mechanics of Materials* **35** (2003) 943-953.

[10] D. N. Fenner, Analogues relating the plane and bending problems for a bimaterial elastic composite, *Journal of Elasticity* **8** (1978) 207-209.

[11] Y. Gu, W. Chen and X. Q. He, Domain-decomposition singular boundary element method for stress analysis in multi-layered elastic materials, *CMC: Computer Materials & Continua* **29** (2012) 129-154.

[12] Y. Gu, W. Chen and C. Zhang, Stress analysis for thin multilayered coating systems using a sinh transformed boundary element method, *International Journal of Solids and Structures* **50** (2013) 3460-3471.

[13] Z. Hashin, Thermoelastic properties of fiber composites with imperfect interface, *Mechanics of Materials* **8** (1990) 333-348.

[14] Z. Hashin, Thin interphase/imperfect interface in elasticity with application to coated fiber composites, *Journal of the Mechanical and Physics of Solids* **50** (2002) 2509-2537.

[15] M. A. Kattis and G. D. Mavroyannis, A unified two-phase potential method for elastic bi-materials: Planar interfaces, *Journal of Elasticity* **103** (2011) 73-94.

[16] I. N. Sneddon, *Fourier Transforms*, Dover Publications, New York, 2003.

[17] L. J. Sudak, On a circular inclusion with an inhomogeneous imperfect interface in plane elasticity, *Mathematics and Mechanics of Solids* **6** (2001) 221-231.

[18] L. J. Sudak and X. Wang, Green's function in plane anisotropic bimaterials with imperfect interface, *IMA Journal of Applied Mathematics* **71** (2006) 783-794.

[19] H. Y. Yu, S. C. Sanday, B. B. Rath and C. I. Chang, Elastic fields due to defects in transversely isotropic bimaterials, *Proceedings of the Royal Society of London A* **449** (1995) 1-30.